Theoretical Studies of Electronic and Nonlinear Optical Properties of Conjugated Polymers

by

Sophia Nicolas Yaliraki

B.A. Harvard University
(1992)

Submitted to the Department of Chemistry
in partial fulfillment of the requirements for the degree of

Doctor of Philosophy

at the

MASSACHUSETTS INSTITUTE OF TECHNOLOGY

June 1997

Author . . . .
Department of Chemistry
May 21, 1997

Certified by . . . .
Robert J. Silbey
Professor
Thesis Supervisor

Accepted by . . . .
Dietmar Seyferth
Chairman, Departmental Committee on Graduate Students

This doctoral thesis has been examined by a Committee of the Department of Chemistry as follows:

Professor Keith A. Nelson ....

Chairman

Professor Robert J. Silbey ....

Thesis Supervisor

Professor Robert W. Field ....

Theoretical Studies of Electronic and Nonlinear Optical Properties of Conjugated Polymers

by

Sophia Nicolas Yaliraki

B.A. Harvard University

(1992)

Abstract

In this thesis we address the relationship of geometric and chemical structure of conjugated molecules and polymers to electronic and optical properties. It is a central question to the problem of characterization and optimization of the nonlinear responses of these materials, which are potential candidates for devices in the new technology of opto-electronics and photonics. Specifically, the effects of conformational disorder on conjugated polymers are studied with an analytical model as well as in simulations. The implications on the conjugation length and the scaling of cubic nonlinearities with the number of double bonds are compared with recent experiments, in which, for the first time problems with solubilities and synthesis have been overcome and the saturation observed.

The effects of an applied field on polyenes with donor-acceptor end groups, where the second order response does not vanish, are examined, to elucidate the origins of a recent proposition, namely that the internal field of the molecule (due to the donor-acceptor as well as the applied electric field) controls its structure and hence the optical response in a simple manner. Both finite and infinitely long systems are studied. The effect of this field to the eigenvalues and eigenstates is dramatic in the infinite system. For finite even membered rings, we find that the field favors the bond alternating chain, and that the critical length where this configuration becomes the stable one, decreases with the field. Only the odd membered radicals, show the simple behavior of structure and optical response proposed.

Finally, a theoretical study of harmonic light scattering (HLS), a reliable and advantageous technique for the measurement of the second polarizability of molecules in solution is presented. The consequences of observing HLS from centrosymmetric molecules are discussed. We propose it is a third order effect, involving γ with the

third field produced by the solvent.

Thesis Supervisor: Robert J. Silbey
Title: Professor

Στους γονείς μου

Acknowledgments

To my advisor, Bob Silbey, I give my warmest thanks for taking me as a student, for guiding me through this thesis, and at the same time giving me freedom to explore my own interests. His excellent taste and knowledge have been invaluable to me. I admire him among other things for his intuition and ability to get to the heart of any problem at once; I am grateful for every piece of advice. His scientific qualities with his personal dignity make him a unique advisor.

Financial support through the Center of Materials Science and Engineering is also gratefully acknowledged.

My current as well as older zoomates have provided a wonderful environment to work hard as well as to joke around at all times: Cliff, Dave, Frank, Joan, Welles; David, Günter, Min of the older generation. I thank them all very much.

I was very fortunate to take my first steps in research as an undergraduate under the guidance of Bill Klemperer. I thank him sincerely for his encouragement and support.

I appreciate all my friends during those years. And, for my family, who has unconditionally been by me in this long path there are not enough words. Such a pity that we had to be apart.

> Let the people who never find true love
> keep saying that there's no such thing.
>
> Their faith will make it easier for them to live and die.
>
> *Wislawa Szymborska*

Contents

Chapter 1

Introduction

The quest for suitable materials to be used in devices in opto-electronics and photonics has been of interdisciplinary interest, in chemistry, physics, and materials science. Since photons can carry information faster, more efficiently and over larger distances than electrons, systems that use light as a carrier of information are of great interest to information and communication technologies. Materials which exhibit high nonlinear optical (NLO) responses are potential candidates for such devices, because they offer the possibility of high speed processing, transmission and storage of data. The nonlinear optical effects, second and third order effects, provide possibilities for optical frequency conversion, optical switching, and optical memory operations [1, 2, 3, 4, 5].

In particular, organic conjugated molecules and polymers have been special candidates as elements in solid-state devices due to their high second and third order responses [6, 7]. They have emerged as a dominant class of photonic materials because they exhibit large and ultra-fast NLO responses, associated with their delocalized π electrons. In addition, they offer advantages to their inorganic counterparts such as thermal and chemical stability, and more possibilities for molecular engineering due to their versatility, either at the backbone or by suitable substitution of side groups or side chains.

Nonlinear optical processes occur when a medium is subjected to an intense electric field $\mathbf{E}$, which polarizes the medium [8, 9]. If the molecule or material lacks a center of symmetry, it is the second-order NLO effects that are of interest; otherwise the first

nonvanishing contribution comes from the third-order contribution. In the dipolar approximation, the induced polarization by an external field is usually written as

$$\mathbf{P} = \alpha \cdot \mathbf{E} + \beta : \mathbf{EE} + \gamma \vdots \mathbf{EEE}$$

where β is a third rank tensor referred to as the hyperpolarizability and γ a fourth rank tensor, the second hyperpolarizability. β and γ constitute the molecular nonlinear responses.

The focus of research then falls broadly in two categories: the systematic characterization of the nonlinear optical properties of materials, as well as the development of reliable experimental techniques for the accurate measurement of NLO properties. The first category encompasses designing optimization strategies of the nonlinear responses. Central to the problem of optimization lies the question of the relation between structure, both chemical and geometric, to the electronic and optical properties, linear and non-linear. Understanding the relationship between geometric and electronic structure enhances the optimization of design strategies. Excellent reviews of theoretical approaches from solid state to quantum chemistry descriptions to the study of the excited states and the spectroscopy of conjugated systems are found elsewhere [10, 11].

In particular, for second order effects (in systems without a center of symmetry), maximum β is believed to occur in systems with large difference of dipole moment between the first excited and the ground state. Thus, the state-of-the art molecules were of the form D-π-A, where an electron donating group, D, was separated from an electron accepting group, A, by a π conjugated system. On the other hand, for third order effects (centrosymmetric systems), the structural requirements are different. The focus has been on the extent of the π conjugation, the effective conjugation length. In both cases, the fundamental question then becomes what limits the magnitude of the nonlinear response.

In this thesis, two essential issues, central to each of the two subcategories just mentioned have been addressed: (a) effects of geometry and conformation changes

to the electronic properties of conjugated systems and thus implications to the effective conjugation length and subsequently to optical properties, and (b) a systematic theoretical study to investigate a recent proposition [12] that β could be correlated with a molecular structural parameter, the bond length alternation, which would then provide the best way to tune β systematically in donor acceptor systems. Finally, the last chapter deals with an experimental technique, reintroduced recently for the measurement of β, namely hyper-Rayleigh light scattering. As such, this work falls in the second broad category of research defined above.

In Chapter 2, the effect of conformational disorder on the electronic and optical properties of conjugated polymers is studied. The magnitude of the cubic nonlinearity γ and its scaling with the number of double bonds of polyenes, the model conjugated system, lie at the heart of understanding the behavior of these systems. Only recently have problems with synthesis and solubilities of conjugated polyenes been overcome and the saturation of γ with chain length been observed for the first time [13]. The onset of this saturation occurs for chain lengths considerably longer than predicted from previous theory, which considered idealized planar, all-trans molecules. We find that, even if deviations from planar configurations are small, the large angular breaks, although rare, are determinative. As a result, the conjugated chain can be described as a succession of relatively long, almost planar segments separated by abrupt breaks or *flips*. It is these flips that dominate the optical properties. Our calculated probability distribution for the segments agrees with results from numerical simulations. When we compare our predictions to the experiment we find that our theory provides better agreement than previous models.

In Chapter 3, the effect of the internal molecular field produced by donor-acceptor groups on the chemical and electronic structure of substituted polyenes is investigated. Large systems are considered through an analytically tractable model. The effect of this field to the eigenvalues and eigenstates is dramatic. It is found to drive the chemical and electronic structure through a structurally observable parameter, the bond order alternation. When we study finite systems, we find that the results of Ref. [12] hold only for odd membered radicals.

In Chapter 4, harmonic light scattering (HLS) of centrosymmetric molecules in solution is studied. The motivation lies in recent propositions of HLS as an advantageous technique for the determination of the hyperpolarizability β of nonlinear optical materials [14, 15, 16]. Unlike the most frequently used method of electric-field induced second harmonic generation (EFISHG), it offers the possibility of experimentally measuring the first hyperpolarizability β of molecules with no ground state permanent dipole moment or of ionic molecules in solution. In the first category lies a new class of molecules which are promising candidates for materials for NLO applications: octupolar molecules; in the second category lie synthetic polymers with NLO chromophores and natural proteins. Both categories are of interest for maximizing the microscopic and macroscopic nonlinear response. We study HLS of centrosymmetric molecules, whose β vanishes identically, and propose that it arises from contributions of the second hyperpolarizability γ and the reaction solvent field. The consequences of this for the determination of β for all types of molecules are discussed. The possibility of hyper-Raman scattering is also examined.

Bibliography

[1] *Frontiers of Polymers and Advanced Materials*, edited by P.N. Prasad, (Plenum, New York, 1994).

[2] For example, Science **263**, 1700 (1994); Chem. & Eng. News **74**, 22 (1996).

[3] *Molecular Nonlinear Optics: Materials, Physics, and Devices*, edited by J. Zyss, (Academic Press, Boston, 1994).

[4] P.N. Prasad and D.J. Williams, *Introduction to Nonlinear Optical Effects in Molecules and Polymers*, Wiley, New York, (1991).

[5] S.R. Marder and J.W. Perry, Science **263**, 1706 (1994).

[6] *Conjugated Polymers: the Novel Science and Technology of Highly Conducting and Nonlinear Optically Active Materials*, edited by J.L. Brédas and R.J. Silbey, (Kluwer, Dordrecht, 1991).

[7] *Nonlinear Optical Properties of Organic Molecules and Crystals*, edited by D.S. Chemla and J. Jyss, (Academic Press, Orlando, 1987), Vol. I and II.

[8] N. Bloembergen, *Nonlinear Optics*, World Scientific, River Edge, NJ, (1996).

[9] Y.R. Shen, *The Principles of Nonlinear Optics*, Wiley, New York, (1984).

[10] Z.G. Soos and G.W. Hayden, in *Handbook of Conducting Polymers*, ed. T.A. Skotheim, Dekker, New York, (1986), p. 197 and references therein.

[11] S. Etemad and Z.G. Soos, in *Spectroscopy of Advanced Materials*, eds R.J.H. Clark and R.E. Hester, Wiley, New York, (1991).

[12] S.R. Marder, C.B. Gorman, F. Meyers, J. Perry, G. Bourhill, J.L. Brédas, B.M. Pierce, Science **265**, 632 (1994); F. Meyers, S.R. Marder, B.M. Pierce, J.L. Brédas, J. Am. Chem. Soc. **116**, 10703 (1994).

[13] I.D.W. Samuel, I. Ledoux, C. Dhenaut, J. Zyss, H.H. Fox, R.R. Schrock, R.J. Silbey, Science **265**, 1070 (1994).

[14] J. Zyss, T. Chau Van, C. Dhenaut, I. Ledoux, Chem. Phys. **177**, 281 (1993).

[15] P. Kaatz and D.P Shelton, Rev. Sci. Instrum. **67**, 1438 (1996).

[16] K. Clays and A. Persoons, Phys. Rev. Lett. **66**, 2980 (1991).

Chapter 2

Conformational Disorder of Conjugated Polymers: Effects on the Conjugation Length and Nonlinear Optical Properties

2.1 Introduction

Conjugated polymers have interesting and, potentially, technologically important electrical and optical properties, such as high conductivity when oxidized, electroluminescence, and large, as well as ultrafast, non-linear susceptibilities [1, 2]. Modern technology focuses on such properties as electrical conductivity and nonlinear optical responses. Organic based nonlinear optical materials are intended for optical switches, light emitting diodes, amplifiers for optical communication and miniature harmonic generators.

The prototype of such conjugated polymer molecules are the polyenes, ranging from small molecules such as hexatriene, octatetraene to carotenes and, finally, to polyacetylene. Because of their relative simplicity these molecules have been the focus of much experimental and theoretical work. The optical properties of short

15

polyenes have been experimentally studied in a series of early papers by Kohler and co-workers [3], and those of polyacetylene by Heeger *et al.* and others ([4] and references therein). Intermediate sized molecules have been rarely studied: experimentally because of the difficulty in their synthesis or solubility, and of their instability, and theoretically, because of computational expense.

In spite of the large body of work, the physical mechanisms underlying certain observed properties are still poorly understood. It is well known that these systems owe their remarkable properties in the delocalized π electrons surrounding the chain backbone, rendering them to virtually 1 dimensional systems. The chains consist of a series of carbon-carbon bonds (e.g. polyacetylene, polydiacetylene) or of a series of aromatic rings (e.g. polyphenylenevinylene, polythiophene, polypyrrole). The electrons occupy two types of orbitals. The σ bond electrons, tied in the covalent C-C bonds along the backbone provide the structural stability and rigidity of the chains; they play very little part in the optical or conducting properties. Each carbon atom in the backbone contributes a p_z orbital involved in the π bonds, which form the extended π electron system, responsible for the different properties of the conjugated polymers in comparison to saturated ones. It is widely accepted that the π electron delocalization length or conjugation length, not necessarily equal to the actual chain length, governs the electronic and optical properties of conjugated systems. This length is related to the average overlap between the π electron orbitals. Nevertheless, the processes which limit or enhance delocalization remain unclear. Furthermore, there is no quantitative agreement on the dependence of properties on the conjugation length.

Theoretical studies of electronic structure and spectra of short polyenes have been carried out by a number of workers [5] using a variety of semi-empirical methods ranging from the Hueckel model (i.e. non-interacting π electrons) to the Pariser-Parr-Pople (PPP) model (interacting π electrons including extended interactions). While the fully interacting model gives an excellent description of the main features of the electronic structure, it is difficult to carry out for systems larger than 10-20 double bonds, and for geometries other than particular ones such as planar all-trans. The

Hueckel model can be solved for any size and geometry in a rather straightforward, albeit tedious manner. However, one can only expect qualitative results from this approach. These considerations have led to the polyenes becoming a "laboratory" for studying one dimensional systems, both theoretically and experimentally.

Ideally, we would like to study the evolution of the optical and electronic properties of oligomers as a function of the number of double bonds. The goal is to guide chemical synthesis of new materials for specific technological applications. Unfortunately, this has been hampered by the inability to synthesize polyene oligomers of known size and good solubility. The latter property is important for the study of single molecule properties, independent of intermolecular interactions that occur in films and which have been absent in all theoretical studies.

Recently remarkable progress in synthesis has led to the discovery of routes to soluble polyenes with double bonds numbering from ~ 25 to > 1000. The evolution of properties with N, the number of double bonds may now be studied. Most emphasis has been put on understanding the behavior of the third order nonlinear response: its magnitude and its scaling with the conjugation length.

The general relation between the induced polarization $\mathbf{P}$ and the applied electric field $\mathbf{E}$ is

$$\mathbf{P} = \chi \mathbf{E}$$

where the macroscopic susceptibility χ is a material dependent parameter. In nonlinear response, χ becomes a field dependent parameter. The polarization induced in the sample by an external electric field is usually expressed in a power series

$$\mathbf{P} = \chi^{(1)} \cdot \mathbf{E} + \chi^{(2)} \cdot \mathbf{EE} + \chi^{(3)} \cdot \mathbf{EEE}.$$

$\chi^{(1)}$ refers to the linear response and $\chi^{(3)}$ corresponds to the macroscopic susceptibility of interest, as centrosymmetric systems have a vanishing $\chi^{(2)}$ due to symmetry. It is the first nonlinear susceptibility that is always allowed. It is usually probed by techniques such as Third Harmonic Generation (THG) where light is emitted at frequency 3ω, from incident radiation of 3 pulses of frequency ω. The correspond-

17

ing microscopic quantity is the molecular second order hyperpolarizability γ. From experiments on small polyenes, it is known that the γ of polyenic systems increases with chain length. Theories show a power law dependence for small N,

$$\gamma = cN^\alpha$$

where α varies from 3 to 6 according to the model(e.g. [6]). For large N, γ is predicted to grow linearly with N, that is γ/N becomes a constant, but there is no agreement on the length where saturation occurs.

The first demonstration of the saturation of the third non-linear optical susceptibility, γ, with increasing N, has been recently reported [7]. Comparison of theory and experiment is difficult because most theoretical studies have been limited to planar all-trans polyenes, while we expect molecules in solution to exhibit "disorder" in the following sense: conformational twists around the single bonds of the backbone will lead to changes in electronic structure and loss of conjugation. There are two limiting theoretical models for this effect: (1) relatively few, strongly disruptive twists leading to a picture of fully conjugated segments of shorter length [8, 9, 10], and (2) relatively many, weakly disruptive twists leading to a wormlike chain [11, 12, 13]. The concept of conjugation length can then be defined for both theoretical models. From theory, we know that, in the case of planar all-trans chains, there is a saturation length, N_s, at which an optical property, for example γ, becomes proportional to N. Thus, for all-trans chains longer than N_s,

$$\gamma = N \frac{\gamma(N_s)}{N_s} = \gamma(N_s) \frac{N}{N_s}$$

so that the chain acts like N/N_s segments of a chain of length N_s. For real chains with imperfections (twists), we may define a conjugation length by comparison to the perfect all-trans chain; that is a real chain of length N may have the properties of N/N_c segments of all-trans chains of length $N_c(N_c < N_s)$. A more likely realization is that an ensemble of real chains of length N will have the properties of a probability distribution $P^N(L)$ of all trans-chains of varying length, L. Depending on the

theoretical model one chooses (worm-like coil or disruptive twists), one will find a different $P^N(L)$.

Another problem in the comparison of theory and experiment has been the size of systems studied. The extrapolation of short-chain results for long chains has been questioned-also the interpolation from the infinitely-long limit has not proved successful.

In this Chapter, we present theoretical studies on long chains to investigate the effects of conformational disorder on the optical properties, such as γ, of long polyene oligomers. The interplay between conformational and electronic degrees of freedom is studied, in an effort to elucidate the connection between chain length and conjugation length and answer an important question: which process limits delocalization of π electrons. Although we only consider optical properties, the role of chain conformation may also be of significance in understanding the transport properties of conjugated polymers. The relation between the way charges are stored (to achieve high conductivity doping is essential) and chain conformation is not yet well understood [14].

We study the conformational behavior of a conjugated polyene chain with allowed rotations around the single bonds. Here, we take into account the electronic transfer and steric repulsions of the system as the most relevant to our purpose. We propose that the chain distorts in a fashion to form numerous almost planar segments (or 'flips'), separated by local breaks caused by large relative angles. Specifically, a number of consecutive double bonds are nearly coplanar with those adjacent until the following one lies in a plane forming an angle of much greater magnitude than the previous one. Then we expect its adjacent double bonds to form another planar segment until a further flip occurs. We.obtain the distribution of such flips, as well as that of the length segments in the chain, both analytically and numerically. Our model differs to that of Rossi *et al.* [10], where they consider a purely phenomenological Hamiltonian of conjugation and steric interactions to obtain conjugation lengths for different types of conjugated polymers.

The effects of conformational disorder on the electronic properties of conjugated

polymers has been the focus of various studies [8, 10, 12, 15, 16]. In some cases, the extent of the effect has been shown theoretically to be small [17], and, since deviations from planar configurations on these systems are small, they have therefore been ignored. Since small deviations from planarity have little effect on the conjugation, and large deviations have a great effect, then for the study of non-linear optical properties, the large deviations, although rare, are determinative. This leads to a model for the optical properties of the conjugated chain that can be described as relatively long, almost planar segments (perhaps "wormlike") separated by abrupt breaks in planarity ("flips"). It is the flips that dominate the optical properties. This is different in spirit to the work of Soos and Schweizer [11], who consider the chain as "wormlike" without large rotational defects that break the conjugation. This alternative description challenges the idea of one effective length as adequate characterization of the properties of conjugated systems. Our work also differs to that of Kohler *et al.* [18], where distributions of conjugation length were varied to best fit measured absorption spectra. Here, we derive a probability distribution of segments beginning from a microscopic Hamiltonian, that we believe contains the most relevant interactions of our problem. This picture leads to an improved explanation of optical properties of long chains as seen in recent experiments [7].

The previous works considering conformational models are briefly summarized: Ref [10] considers a purely phenomenological hamiltonian and does not consider optical properties, while the work in Ref [15] involves simulations of a Hueckel Hamiltonian which includes rotational degrees of freedom. The focus is mainly on spectrum modifications and, opposite to Ref. [10] on the fermionic part. Finally, in the work of Ref [11] only the weak disorder limit is considered, so that only dipole transition moments are affected and not the energy levels.

We consider systems with alternating single and double bonds. Rotation around each single bond is allowed; a plane or platelet is associated with each double bond. Although we choose polyacetylene to illustrate the model, we are not confined to this system. Any monomeric unit, such as a ring, can be the building block of the platelet. Each platelet forms an angle θ with the reference plane of the perfectly
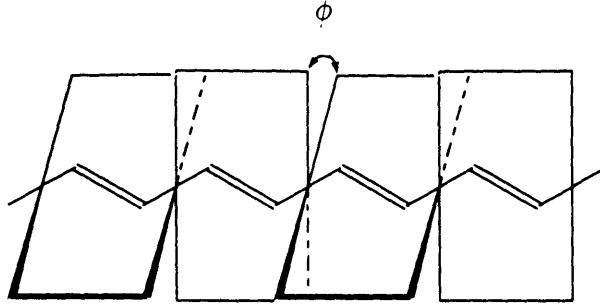
Figure 2-1: Model system: adjacent platelets form a relative angle ϕ.

planar chain; adjacent platelets form a relative angle ϕ (Figure 2-1). A tight binding model with modified transfer integrals (to accommodate rotations) is used to describe the electronic behavior of the system. A torsional potential takes into account steric effects arising from the rotation of platelets. Electron correlations are ignored at this level. We show that the 'fragmented' chain constitutes a meaningful picture for these systems, and apply it to the calculation of optical properties such as the absorption spectrum, the linear polarizability, α, and the second hyperpolarizability, γ. We also study the effect of conformational disorder for this system through numerical simulations, using a Metropolis type algorithm. We compare our analytical results to those from the simulations as well as to experiments and show good agreement.

The Chapter is structured as follows: in Section 2.2 we present the microscopic model Hamiltonian of conjugation and steric interactions. We derive from this Hamiltonian the phenomenological term used by Rossi et al. [10] to model torsional motion. In Sections 2.3 and 2.4 we discuss the picture of the fragmented chain. In Section 2.3 we calculate the number of flips in the chain from the phenomenological model, as well as the probability distribution of the length of the conjugated segments between flips. In Section 2.4 we discuss our numerical simulations performed with the original microscopic Hamiltonian and compare with the analytical results. Finally in Section 2.5 we calculate optical properties based on the results of our model in Section 2.3 and compare with experiments.

2.2 The model

We study the conformational behavior of a conjugated chain with allowed rotations around the single bonds, taking into account both the electronic transfer terms and steric repulsion interactions in the system as the most relevant to our purpose. It is widely accepted that, due to steric interactions, delocalization of electrons is hindered, although the manner and extent of this is yet to be fully understood. As noted above, we propose that a long chain does not distort in a continuous wormlike manner, but rather, in a disjointed fashion, forming numerous smaller than original length, almost planar segments (also referred to as 'strings'), separated by sudden, local breaks (or 'flips') caused by large relative angles. Specifically, a number of consecutive platelets are coplanar (to within a small angle) with those adjacent until the next one lies in a plane forming an angle of much greater magnitude than the previous ones. Then the adjacent platelets form another almost planar string until a further flip occurs, producing a distribution of angles between platelets mainly concentrated around zero, occurring in clusters, with a few outside of that range. Thus the long chain can be considered to be a collection of quasi-planar segments separated by large angle flips. The optical properties are dominated by the distribution of segment lengths; thus the precise distribution of angles within a segment is unimportant. To substantiate the proposed picture, we calculate the probability distribution of such breaks or 'flips', as well as the number and length of planar segments or 'strings' in a chain of total $2N$ carbon atoms,and we compare the results with numerical experiments on the same systems. Within this picture, we are able to account for aspects of the experimental behavior of the third order polarizability γ of such conjugated systems [7]. The implication of such an approach suggests that the idea of a single effective length for a given chain is inadequate. The chain behaves in effect, not as one of smaller than original length, but as a collection of smaller ones. In this study we neglect interactions between those segments. Also, the length of these segments may not be constant, but may change together with the configuration of the chain with time evolution. However, the ensemble of chains has a stationary probability distribution.

Our simulations, discussed in Section 2.4 are in good quantitative agreement with this model. Note the similarity of this picture to that of Schweizer who studied linear optical properties and phase transitions in polymers [13].

We now introduce the microscopic Hamiltonian of our system. A chain of $2N$ atoms with one unpaired electron per atom is considered. The chain is treated as a one dimensional system with $2N$ sites, each occupied by an atom. The most relevant interactions for our problem are the steric interactions between adjacent groups, which tend to keep adjacent platelets away from planarity, and the delocalization of electrons, which favors the planar conformation. The electron-phonon coupling interaction is explicitly neglected, although bond dimerization is imposed. Electron-electron interactions are not considered at this stage; however we expect that they reduce delocalization, thus making the steric effect even more important and our picture more relevant.

The Hamiltonian

$$
\begin{aligned}
H = \ & - \ \sum_{\sigma} \sum_{n=1}^{N} [t_d c_{n\sigma,1}^{\dagger} c_{n\sigma,2} + t_s \cos(\theta_n - \theta_{n+1}) c_{n\sigma,2}^{\dagger} c_{n+1\sigma,1} \\
& + \ \mathrm{h.c.}] - \sum_{n=1}^{N} V_o \cos(\theta_n - \theta_{n+1})
\end{aligned}
\tag{2.1}
$$

describes the conjugation and the steric effect. Each of the N unit cells contains two carbon atoms - a double and a single bond of fixed length. The standard fermionic operators $c_{n\sigma,a}^{\dagger}$ ($c_{n\sigma,a}$) create(annihilate) an electron of spin σ on position a of unit cell n. t_s and t_d are the electron transfer integrals for single and double bonds respectively. They can be obtained from experimental observation of the band gap through an electron-phonon coupling model like that of Su-Schrieffer-Heeger [19]. Notice that transfer across a single bond depends on the relative orientation of the neighboring platelets. V_o represents an effective steric hindrance energy parameter. If the interaction is favorable, as for example in hydrogen bonding cases, $V_o > 0$; if the steric interactions are repulsive, then either $V_o < 0$ or we can consider a term of the form $\cos(\pi - \Delta\theta) = -\cos(\Delta\theta)$.

Our model stresses the competition between conjugation and steric interactions.

We should emphasize though that, in contrast to Rossi *et al* [10], we begin from a microscopic description instead of using a phenomenological model . Rossi *et al* study the role of conformational disorder of such systems with the use of effective potentials,

$$H_R = \sum_{n=1}^{N} -E_c \cos 2(\theta_n - \theta_{n+1}) - E_s \cos(\theta_n - \theta_{n+1}) \qquad (2.2)$$

$$= H_{conj} + H_{ster}.$$

The form of the conjugation term agrees with our intuitive understanding: it exhibits a minimum when the platelets are aligned, and a maximum when they are perpendicular to each other. By a simple change of variables $\phi_n = \theta_n - \theta_{n+1}$, with Jacobian equal to unity, we can transform both Hamiltonians to relative angle of platelets variables,$\{\phi_i\}$.

We now derive the phenomenological Hamiltonian (Eq. (2.2)) from the microscopic Hamiltonian (Eq. (2.1)). Starting from the electronic part of our model(Eq. (2.1)), through a perturbation expansion for small angles, we derive the angular dependence for the conjugation energy. Since the first term of Eq. (2.2) represents the change in conjugation energy caused by a conformational change, this provides justification for the use of such widely used phenomenological potentials and relates it analytically to the ratio of transfer integrals. We also show numerically, for all angles, agreement with the E_c value and with the $\cos(2\phi)$ functional dependence.

We assume that all the platelets are aligned with each other except for the two in position n_p and n_{p+1} *i.e.*all ϕ_n are set to zero except for those two such that they form an angle $\phi_{n_p} = \theta_{n_p} - \theta_{n_p+1}$. Note that if the minimum energy angle is not $\phi = 0$, but ϕ_{eq}, we can expand around ϕ_{eq} instead of $\phi = 0$. The subsequent argument is unaffected. Assuming the angles are small enough to allow for an expansion of the $\cos \phi$, the first term of the Hamiltonian can be expressed in the following manner:

$$H = H_o + V(\phi)$$

$$H = -\sum_\sigma \sum_{n=1}^N \{t_d c_{n\sigma,1}^\dagger c_{n\sigma,2} + t_s c_{n\sigma,2}^\dagger c_{n+1\sigma,1} + \text{h.c.}\}$$
$$+ \sum_\sigma \frac{t_s}{2} \phi_{n_p}{}^2 c_{n_p\sigma,2}^\dagger c_{n_p+1\sigma,1} + \text{h.c.}$$

where H_o is the standard tight binding Hamiltonian with known exact analytic solutions for periodic boundary conditions. $V(\phi)$ can be viewed as the perturbative effect of conformational disorder on conjugation and is thus related to the phenomenological term of H_R. After making the approximation for small angles and requiring it to hold for all angles ϕ,

$$< G_o|V|G_o > = < G_o|\sum_\sigma \frac{t_s}{2}\phi_{n_p}{}^2 c_{n_p\sigma,2}^\dagger c_{n_p+1\sigma,1} + \text{h.c.}|G_o >$$
$$= 2E_c\phi^2 \cong E_c(1 - \cos 2\phi)$$

where $|G_o >$ is the ground state eigenfunction of the standard Hamiltonian H_o. Exploiting the periodic boundary conditions, H_o can be diagonalized with the following operators keeping in mind that there are two carbon atoms per unit cell

$$c_{k\sigma,a} = \frac{1}{\sqrt{N}} \sum_n e^{-ikn} c_{n\sigma,a}$$

$$k = 2\pi j/N, \qquad j = 0, 1, .., (N - 1)$$

and $a = 1, 2$ stands for the position of a carbon atom in the unit cell. H_o now becomes

$$H_o = -\sum_{k,\sigma} (c_{k\sigma,1}^\dagger, c_{k\sigma,2}^\dagger) \begin{pmatrix} 0 & t_d + t_s e^{-ik} \\ t_d + t_s e^{ik} & 0 \end{pmatrix} \begin{pmatrix} c_{k\sigma,1} \\ c_{k\sigma,2} \end{pmatrix}$$

and can be brought to diagonal form with the standard transformation

$$T = \begin{pmatrix} e^{i\alpha_k} \cos\theta_{k\sigma} & -e^{i\alpha_k} \sin\theta_{k\sigma} \\ \sin\theta_{k\sigma} & \cos\theta_{k\sigma} \end{pmatrix}$$

with

$$\tan\alpha_k = -\frac{t_s \sin k}{t_d + t_s \cos k} \tag{2.3}$$

25

and $\theta_{k\sigma} = \pi/4$. The Hamiltonian H_o can be expressed in terms of new operators

$$H_o = -\sum_\sigma \sum_{i=1,2} \sum_k E_{k\sigma,i} b^\dagger_{k\sigma,i} b_{k\sigma,i}$$

with

$$E_{k\sigma,j} = (-1)^j (t_d{}^2 + t_s{}^2 + 2t_s t_d \cos k)^{1/2}$$

and

$$\begin{pmatrix} b_{k\sigma 1} \\ b_{k\sigma 2} \end{pmatrix} = T^{-1} \begin{pmatrix} c_{k\sigma,1} \\ c_{k\sigma,2} \end{pmatrix}$$

The ground state $|G_o> = \prod_{k=0,\sigma}^{\leq \pi} b^\dagger_{k\sigma,1}|0>$ where $|0>$ is the vacuum state, and $b^\dagger_{k\sigma,1} = \frac{1}{\sqrt{2}}(c^\dagger_{k\sigma,1} e^{i\alpha_k} + c^\dagger_{k\sigma,2})$. By expressing V in terms of the new operators $b_{k a}$, we obtain the energy correction

$$E_c = \frac{t_s}{N} \sum_k \cos(\alpha_k + k).$$

From Eq. (2.3),

$$\cos\alpha_k = \frac{\frac{t_d}{t_s} + \cos k}{\left[1 + \frac{t_d}{t_s}^2 + 2t_s t_d \cos k\right]^{1/2}},$$

$$\sin\alpha_k = \frac{-\sin k}{\left[1 + \frac{t_d}{t_s}^2 + 2t_s t_d \cos k\right]^{1/2}}.$$

Using the trigonometric identity for sums of cosines,

$$E_c = -\frac{t_s}{2N} \sum_k \frac{\frac{t_d}{t_s} + \cos k}{\left[1 + \left(\frac{t_d}{t_s}\right)^2 + 2\frac{t_d}{t_s} \cos k\right]^{1/2}}.$$

Approximating the sums with integrals, we obtain

$$E_c = \frac{t_s}{4\pi} \left[\frac{1}{\frac{t_d}{t_s} + 1} K(r) + \frac{t_d}{t_s}\left(1 + \frac{t_d}{t_s}\right)^2 E(r) - \left(1 + \frac{t_d}{t_s}^2\right) K(r)\right]$$

where $E(r)$ and $K(r)$ are the complete elliptic integrals of the first kind and second

kind respectively with argument

$$r = \frac{2[\frac{t_d}{t_s}]^{1/2}}{1 + \frac{t_d}{t_s}}.$$

As the physically relevant range occurs when the ratio r approaches one, we consider this limiting behavior of the elliptic integrals. For r close to one, $K(r)$ approaches $\frac{1}{2}ln(\frac{16}{1-r})$, and $E(r) \simeq \frac{1}{2}ln(\frac{16}{1-r}) - 1$. After some algebra, we find

$$K(r) = ln4 + ln(\frac{\frac{t_d}{t_s} + 1}{\frac{t_d}{t_s} - 1}) = ln4 + 2\coth^{-1}(\frac{t_d}{t_s}.)$$

Similarly, $E(r) = ln4 + 2\tanh^{-1}(\frac{t_d}{t_s}) - 1$. Finally, we set $t \equiv \frac{t_d}{t_s}$, and we obtain

$$E_c = \frac{t_s}{4\pi}[\frac{ln4 + 2\coth^{-1}(t)}{1 + t} + 2t^2(ln4 + 2\coth^{-1}(t)) - t(1 + t)^2]. \qquad (2.4)$$

We notice immediately the dependence of the conjugation energy per units of t_d on the ratio, t, of the transfer integrals. According to standard mean field theories (e.g. [19]) this ratio depends only on the band gap E_g and band width W_g of the system

$$t_d/t_s = \frac{1 + E_g/W_g}{1 - E_g/W_g}.$$

We are thus able to connect our microscopic model to a phenomenological one whose parameters can be obtained from experimental data. By using the "standard" values for $E_g = 1.4$ eV and $W_g = 10$ eV (and $t_s = 2.15$ eV, $t_d = 2.85$ eV) for polyenes, we obtain for $E_c/N = 0.015$ eV. To check the validity of our approximations, we numerically performed the same calculation with the original Hamiltonian, and obtained the same value for E_c.

Having made the above connections, we can use the H_R Hamiltonian of Eq. (2.2) to study the chain under conformational disorder. Estimates for the effective steric potential parameter in solution are based on NMR spectroscopy and in the gas phase on Raman spectroscopy, as well as *ab initio* or semiempirical calculations. For example, for polyacetylene Rossi *et al.* used the value $E_s = 1.5$ kcal/mol, as estimated

in Ref. [20]. Here, we do not consider any particular system and we take $V_o = .026$ eV, a room-temperature value. This value should be appropriately changed for each polymer.

2.3 Fragmentary versus wormlike chain

2.3.1 Calculation of number of flips in a chain

To distinguish between a wormlike and a fragmentary chain, we would like to know how many abrupt changes occur in equilibrium conformations of the system. The definition of an abrupt change may seem rather arbitrary, but our results turn out to be insensitive to its absolute measure within broad limits. Crudely, one can think of bonds as completely conjugated ($\theta_i - \theta_{i+1} = 0$) or completely broken ($\theta_i - \theta_{i+1} = \pi/2$). We consider a more realistic situation: a "flip" occurs when $|\theta_i - \theta_{i+1}| > \phi_0$. In the simulations on polyacetylene, discussed in detail in Section 2.4, ϕ_0 is taken to be $10, 15$ and 20 degrees without qualitative difference in the results. We thus proceed to calculate the probability distribution as well as the most probable number of flips in a chain of N double bonds, using the H_R Hamiltonian (Eq. 2.2).

Our model only includes nearest neighbor interactions- the relative angles of platelets are thus independent variables. The probability distribution of any angle ϕ_i is

$$P(\phi) = \frac{e^{\beta(E_c \cos 2\phi + E_s \cos \phi)}}{Z}$$

where $\beta = \frac{1}{kT}$ and $Z = \int_{-\pi}^{\pi} d\phi e^{E_c \cos 2\phi + E_s \cos \phi}$. For systems which favor a planar conformation, we expect the angles to be small, so we expand the Hamiltonian around the minimum $\phi = 0$, (if $\phi_{eq} \neq 0$, an expansion is made around ϕ_{eq})

$$H_R = \sum_{i=1}^{N} -E_c(1 - 2\phi_i^2) - E_s(1 - \phi_i^2/2).$$

The angle dependency is usually ignored because its effect on electronic properties is negligible. We will show however that, no matter how small, these angular deviations

give rise to a new physical picture. A similar approach can be taken for chains with a minimum configuration other than the perfectly planar one and the qualitative behavior is the same. The probability distribution now becomes

$$P(\phi) = \frac{e^{-\beta\phi^2(E_s+4E_c)/2}}{\int_{-\pi}^{\pi} d\phi e^{-\beta\phi^2(E_s+4E_c)/2}}. \tag{2.5}$$

We can now obtain from Eq. (2.5) the probability of two adjacent platelets being coplanar, and we find it to be $P(0) = 0.72$. From the numerical simulations (Section 2.4), we also observe approximately 70% of the angles to be around zero. Such clustering of the relative angles of platelets around zero reinforces the fragmented chain picture.

We now calculate the most probable number of flips or breaks, m^*, in conjugation in the chain. Consider an open chain, so there are N-1 single bonds. If all platelets were coplanar, the energy of the system would be

$$E = -(N-1)(E_s + E_c).$$

If one flip occurs, then $E = -(N-2)(E_s + E_c) - E_s\cos\phi - E_c\cos 2\phi$. For m flips,

$$E = -(N-m-1)(E_s + E_c) - \sum_{i=1}^{m}(E_s\cos\phi_i + E_c\cos 2\phi_i).$$

So

$$\begin{aligned}
Z &= \sum_m e^{(N-m-1)(E_s+E_c)/kT} e^{\beta\sum_{i=1}^{m}(E_s\cos\phi_i+E_c\cos 2\phi_i)} C_m^N \\
&= \sum_m T_m
\end{aligned}$$

where $C_m^{N-1} = \frac{(N-1)!}{m!(N-m-1)!}$ takes into account the different ways m flips can occur in $N-1$ possible sites. In Figure 2-2, we notice that this distribution of flips agrees very well with that obtained from the results of numerical experiments described in detail in Section 2.4.

After making Stirling's approximation, we obtain for the most probable number
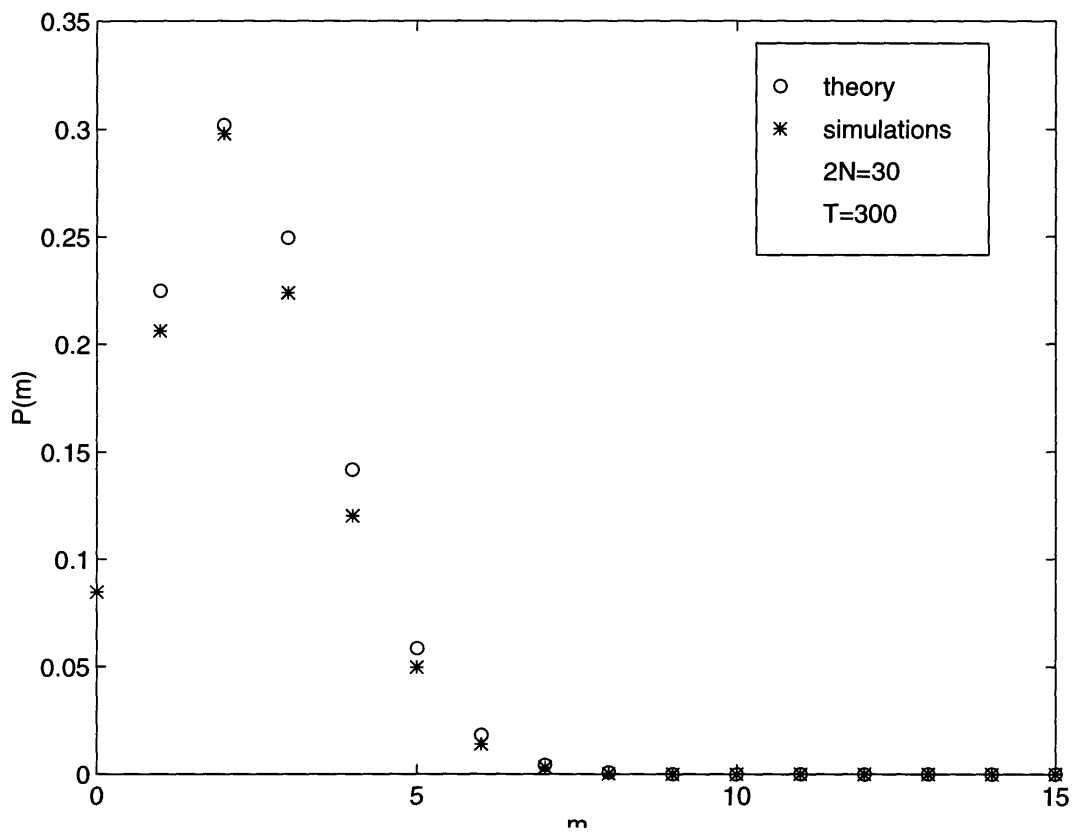
29

Figure 2-2: Probability distribution of "flips" in a chain of 30 carbon atoms at $T = 300$ K from theory and simulations

T in K	m^*_{calc}	m^*_{sim}
300	3	2
400	4.5	3
600	7	5

Table 2.1: Most probable number of flips in a chain of 30 carbon atoms from theory and simulation.

of flips , m^*,

$$\frac{dT_m}{dm} = 0 \Rightarrow \frac{m^*}{N} \simeq e^{-(E_s+E_c)/kT}. \qquad (2.6)$$

Since E_s is directly related to V_o and E_c to $\frac{t_d}{t_s}$ according to relation (4), our result is immediately connected to our original model. Note that as the temperature T increases, more flips are expected to occur. Similarly, a longer chain can support more flips. These results agree with intuitive ideas of increasing disorder with increasing temperature, as well as higher number of conformational distortions at longer lengths. Additionally, we can see from the above formula that as N increases, one expects to find more planar segments (strings), instead of longer ones. So the probability distribution of lengths of the strings will eventually be independent of N. We compare the values of the most probable number of flips for a chain of 30 atoms at different temperatures between predictions of the model and numerical experiments, (see Section 2.4), and find relatively good agreement. Since the long chain limit has been invoked, we expect an even better agreement for longer chains. As can be seen in table 1, the number of flips is substantial, supporting the idea of a fragmented chain.

2.3.2 Calculation of distribution of length segments, $\wp^N(\ell)$

We are also interested in the probability of finding a fully conjugated segment of length ℓ between flips in the chain. We consider such strings to be fully conjugated when the angular difference of adjacent platelets is small, i.e.

$$|\phi_i| \leq \phi_0$$

31

for all i within the segment. Determining this probability distribution, $\wp^N(\ell)$, is important because it will enable the calculation of experimental physical properties of these systems, such as the absorption spectrum, the linear polarizability, α, and the second hyperpolarizability, γ, described in Section 2.5.

In general, for any property, x, its average $< x >$ can be obtained from the probability distribution $\wp^N(\ell)$ in the following way: if we consider an ensemble of Z molecules, each with N double bonds, then

$$< x > \; = \; \frac{1}{Z} \sum_{all\, seg,\, all\, mol} x = \frac{1}{Z} \sum_\ell N(\ell) x(\ell)$$

$$= \; \frac{1}{Z} \sum_\ell N_{tot,seg} \wp^N(\ell) x(\ell) \tag{2.7}$$

where $\wp^N(\ell) = N(\ell)/N_{tot,seg}$, with $N(\ell)$ the number of segments with length ℓ in the ensemble and $N_{tot,seg}$ the total number of segments. Finally,

$$\frac{< x >}{N} =< \frac{1}{\ell} > \sum_\ell \wp^N(\ell) x(\ell), \tag{2.8}$$

where $< \frac{1}{\ell} >$ is $1/N$ times the average number of segments per molecule or $\sum_\ell \frac{\wp^N(\ell)}{\ell}$.

We now proceed to calculate $\wp^N(\ell)$. Consider an open chain with N double bonds and k breaks, or "flips" as defined above, in the $N - 1$ single bonds so that $k + 1$ segments constitute the chain. The ith segment has length n_i. The probability of having a segment of length ℓ in this molecule, is $P_k^N(\ell)$, is given by

$$P_k^N(l) = M_k^N \sum_{n_1=1}^{N} \sum_{n_2=1}^{N} \cdots \sum_{n_{k+1}=1}^{N}$$

$$\delta[N - \sum_{i=1}^{k+1} n_i]\{\delta(n_1 - l) + \ldots + \delta(n_{k+1} - l)\}$$

with normalization factor M_k^N. Recognizing that all terms are equivalent, and using the exponential form of the delta function we obtain

$$P_k^N(l) = M_k^N(k + 1) \sum_{n_2} \cdots \sum_{n_{k+1}} \int_0^{2\pi} exp[i\theta(N - l - \sum_2^{k+1} n_i)] \frac{d\theta}{(2\pi)}.$$

After performing the summations and some algebra,

$$P_k^N(\ell) = M_k^N(k+1)\frac{(N-1-\ell)!}{(N-k-\ell)!}.$$

To obtain the normalization factor from $\sum_{\ell=1}^{N-k} P_k^N(\ell) = 1$, we redefine $M_k'^N = M_k^N(k+1)$, and use $\sum_{\ell=1}^{N-k} \frac{(N-\ell-1)!}{(N-k-\ell)!} = \frac{(N-1)!}{k(N-k-1)!}$. Finally,

$$P_k^N(l) = \frac{k(N-k-1)!(N-l-1)!}{(N-1)!(N-k-l)!} \qquad for \qquad k \neq 0$$

and

$$P_0^N(\ell) = \delta_{N,\ell}.$$

The total probability of having a segment of length ℓ, is $P_k^N(\ell)$ multiplied by the probability of k breaks in a length of N double bonds, which is given by $C_k^{N-1}p^{N-1-k}q^k$ (C_k^{N-1} being the same binomial coefficient as previously). Therefore,

$$\wp^N(l) = \sum_{k=1}^{N-l} p^{N-1-k}q^k \frac{(N-1-\ell)!}{(N-l-k)!}\frac{k(N-1-k)!(N-1)!}{(N-1)!(N-1-k)!k!}. \tag{2.9}$$

p here corresponds to having two consecutive coplanar platelets, and, similarly, $q = 1-p$ to having a flip or break in conjugation.

Simplifying the equation and renaming $\kappa = k-1$, we obtain

$$\wp^N(l) = p^{N-2}q \sum_{k=0}^{N-l-1} \left(\frac{q}{p}\right)^k C_k^{N-l-1}$$

$$= p^{N-2}q\left(1+\frac{q}{p}\right)^{N-l-1} = \frac{p^{N-2}q}{p^{N-l-1}}(p+q)^{N-l-1}$$

$$\wp^N(l) = p^{l-1}q \tag{2.10}$$

Since p is the probability of having two single bonds coplanar, it can be related to the number of flips in the chain in the following way:

$$p = \frac{N-1-m^*}{N-1},$$

where m^* is the most probable number of flips in a chain of $N - 1$ single bonds. If the large N limit is assumed, m^* is given by Eq. (2.6), so that

$$p = \frac{N - 1 - Ne^{-(E_s + E_c)/kT}}{N - 1}.$$ (2.11)

Comparison with simulations (Section 2.4) is good as can be seen in Figures 2-3 and 2-4. As expected, there is better agreement with increasing N.

2.4 Simulations

In addition to the analytical model described above, the effect of conformational disorder on conjugated systems and their optical properties was also studied through numerical simulations. To test the validity of the fragmentary chain picture we used the full Hamiltonian of Eq. (2.1). We find that the results of those simulations agree with the predictions of our analytical model. A Metropolis algorithm [21] was employed - instead of choosing configurations randomly and then weighing them with a Boltzmann weight, we choose them with a probability $e^{-\beta H}$ and then weigh them equally. Configurations are produced by randomly moving one angle at a time in succession along the chain. The total energy is calculated by diagonalizing the Hamiltonian of Eq. (2.1) for that configuration. The average of any property, y, is then

$$< y > = 1/M \sum_{i=1}^{M} y_i$$ (2.12)

where y_i is the value of the property y of the ith configuration. M is the total number of configurations. Typically, M is $5000N$ in our case. The first configuration is randomly generated and configurations contribute to averages only after "equilibrium" is reached. From the equilibrium configurations, we extract information about the chain distortion. For the cases we considered, the notion of the fragmentary chain is appropriate: first, we observe that the overwhelming majority of angles is indeed close to zero as discussed in the previous Section. We found flips as defined in Section 2.3 and almost planar segments between flips. A typical configuration for $N = 45$ can be
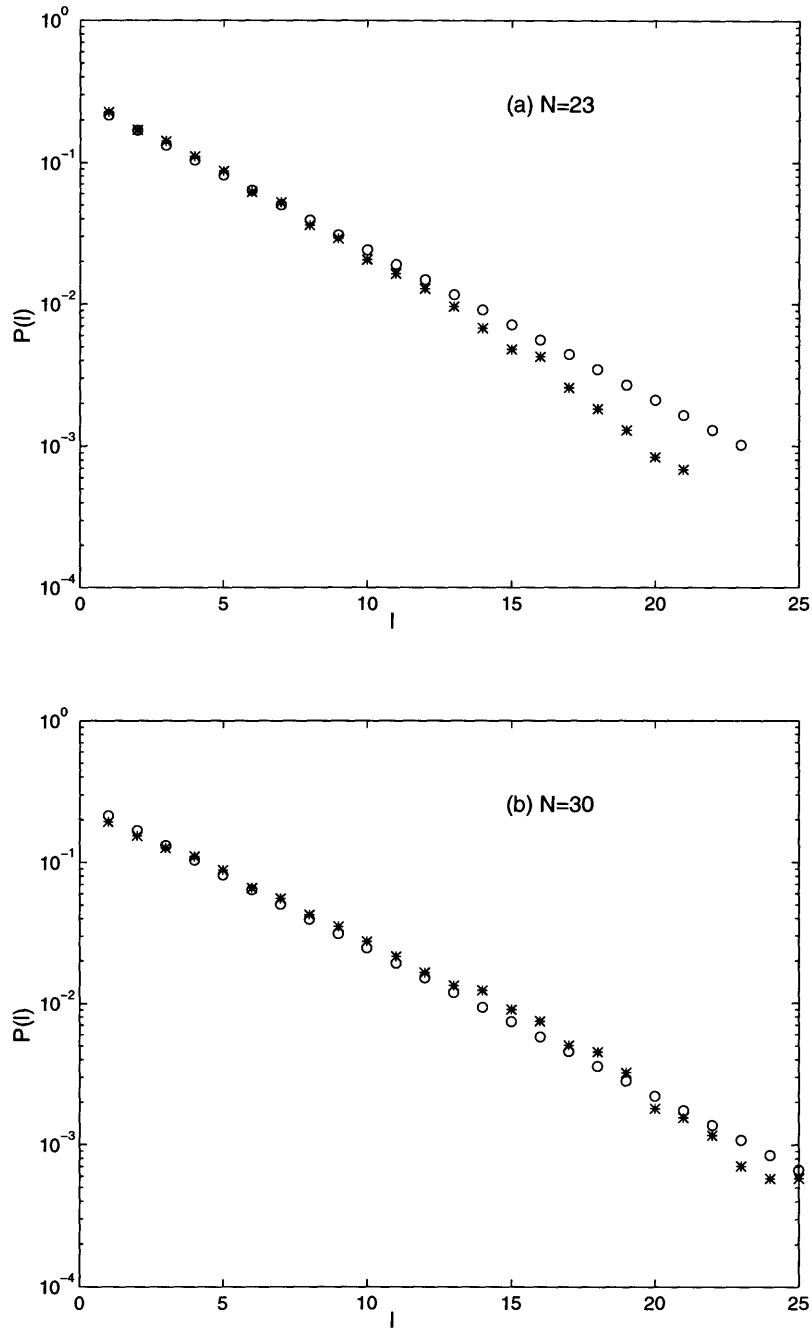
Figure 2-3: Probability distribution of a segment of ℓ double bonds in chains of (a) $N = 23$, (b) $N = 30$ double bonds from theory (o) and simulation (*).
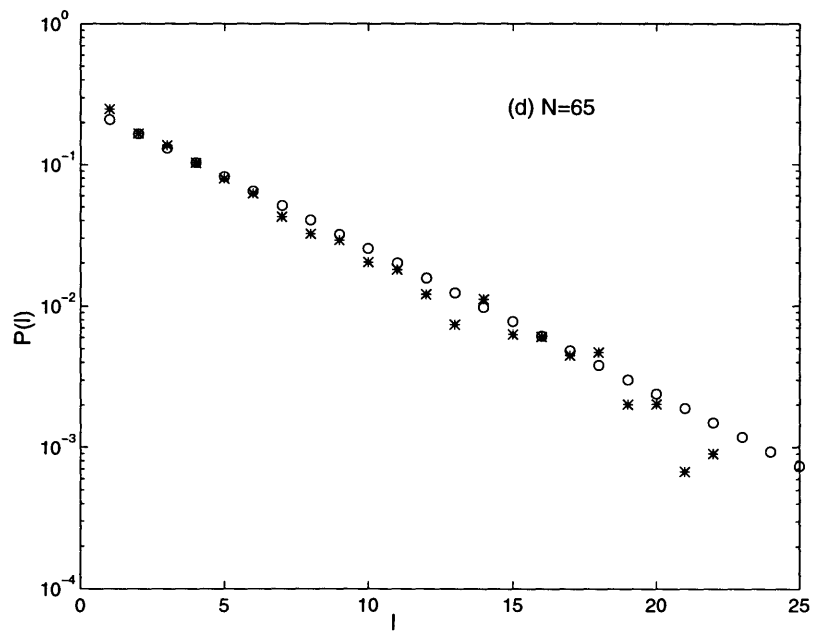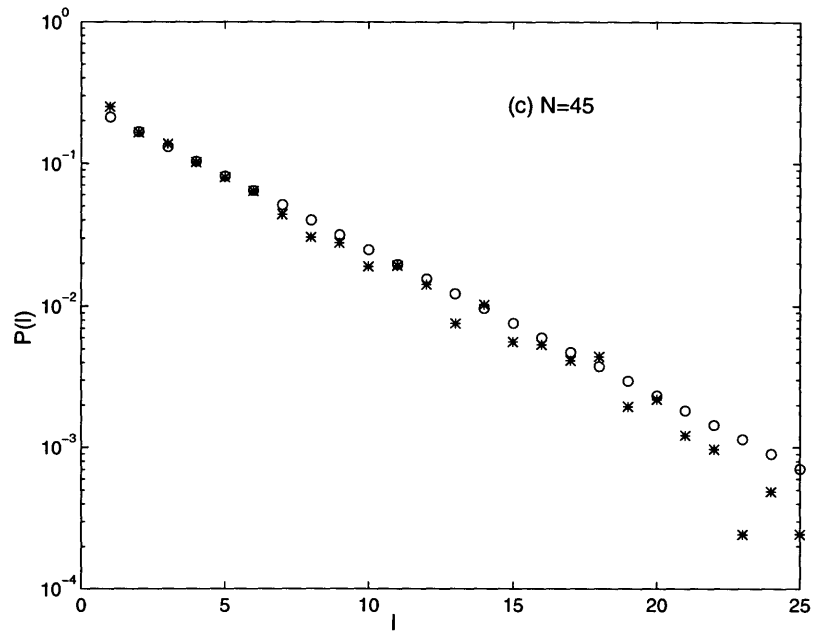
Figure 2-4: Probability distribution of a segment of ℓ double bonds in chains of (c) $N = 45$, (d) $N = 65$ double bonds from theory (o) and simulation (∗).
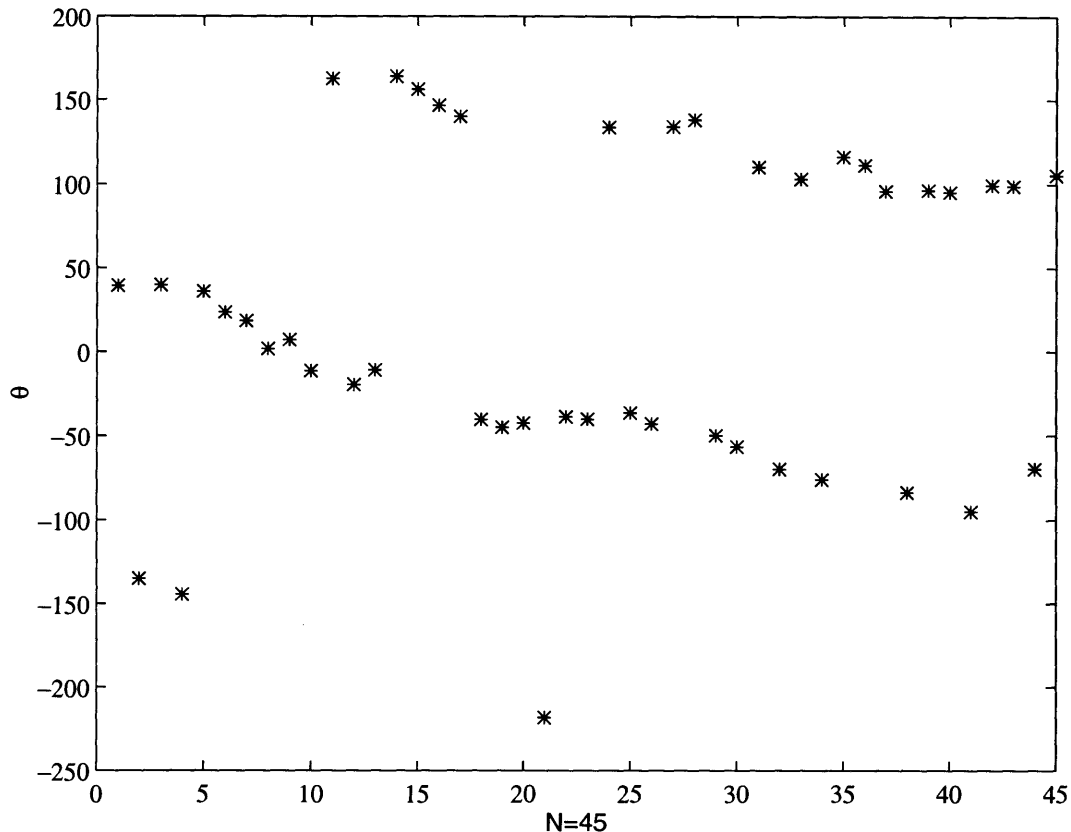
Figure 2-5: Typical configuration of a chain of 45 double bonds from the simulations.

seen in Figure 2-5. Note the appearance of flips.

We performed the simulations at three different temperatures, $T = 300, 400, 600K$; for five different ratios of transfer integrals t_s/t_d from 0.3 to 0.8; for values of the steric energy parameter V_o between 0.026 and 0.0033 eV; and for chains between 30 and 130 C atoms.

We also calculated the linear polarizability α. For each configuration, we use the standard expression from perturbation theory

$$\alpha = 2 \sum_n{}' \frac{< G|\mu|n >< n|\mu|G >}{E_n - E_G} \qquad (2.13)$$

where $< G|\mu|n >$ is the transition moment matrix element between an excited and the ground state, and we obtain the average according to Eq. (3.7). All matrix elements are computed within the tight-binding approximation. With a centrosymmetric position system and within the one electron approximation, $< G|\mu|n >$ becomes

37

$\sum_i c_i^{\dagger ho} c_i^{el} z_i$ where z_i is the distance of site i from the origin - the center of the chain in our case- and $c_i^{\dagger ho} c^{el_i}$ the eigenfunctions of the hole and the electron respectively of the excited state $|n >$. The original choice for V_o, t_s, and t_d, as commented in Section 2.2, is .026, 2.15, and 2.85 ev respectively. Note from Figure 2-6 the striking dependence of the linear polarizability to the transfer integrals ratio, and the insensitivity to the steric parameter. This is fortunate since the transfer integrals can be computed from experimental measurements of the band gap and band width, while the steric parameter determination is based on cruder methods. The dependence on the ratio of transfer integrals is evident in our calculations of Section 2.3.
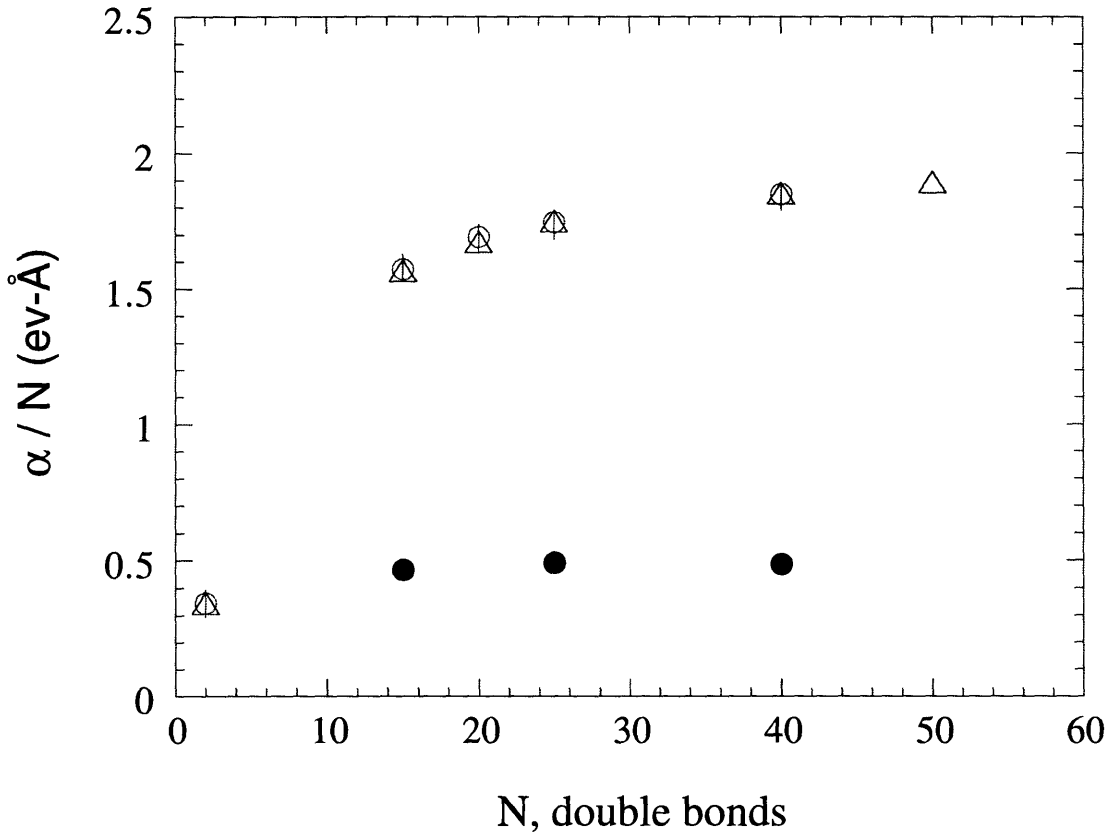

Figure 2-6: α/N from simulations. (o) $V_o = 0.026$ eV, $t_s = 2.15$ eV, $t_d = 2.85$ eV. ($\triangle$) $V_o/2$, (|) $V_o/4$, ($\bullet$) V_o, $0.71\,t_s = 1.52$ eV.

2.5 Optical properties: α, γ and absorption

With an analytical expression for the probability of occurrence of a planar segment of length ℓ in a chain of N double bonds, we can calculate any physical property of the system and compare with numerical simulations and experiments to test the relevance and applicability of the proposed picture of the chain as a collection of small planar segments. Extensive discussion of the optical properties can be found elsewhere [22]. Here we will comment only briefly on optical properties, since they will be discussed in a forthcoming paper. We will show that there is agreement with numerical experiments, and that we are able to explain many of the features of recent experiments on long chains [7].

We calculate these properties according to our proposed model of Eq. (2.8), as was explained in Section 2.3. Here, $x(l)$ is the value of the property of a completely planar all trans chain with $2l$ carbon atoms. For $\alpha(\ell)$, we use the expression of Eq. (3.6). For $\gamma(\ell)$, we follow the approach of Yaron *et al.* [23].

We compare with the simulations in the following way: we use the configurations generated by the simulations, after diagonalization of the electronic and steric Hamiltonian of Eq. (2.1), and calculate α in the manner explained in Section 2.4 and γ according to Ref.(11). We compare with the predictions of our analytical model, which uses the probability distribution of Eqs. (2.10)- (2.11). The values of the parameters are again: $V_o = 0.026$ ev, $t_s = 2.15$ ev and $t_d = 2.85$ ev. The agreement can be seen in Figures2-7 and 2-8. Our analytical model captures the behavior of the system.

When we compare our results with that of recent experiment [7], we can immediately see that our saturation value for γ/N is close to the experimental value $(14.5 \times 10^{-34}$ vs 16×10^{-34} electrostatic units(esu) respectively). In our model, the saturation is reached for chains of ≈ 80 carbons (40 double bonds), longer than theoretically predicted for the fully planar all trans molecule ($\approx 20 - 30$ double bonds)[23, 24, 25], and shorter than seen in the experiment (saturation at 240 carbons). This latter discrepancy has been now partly resolved due to new mass mea-
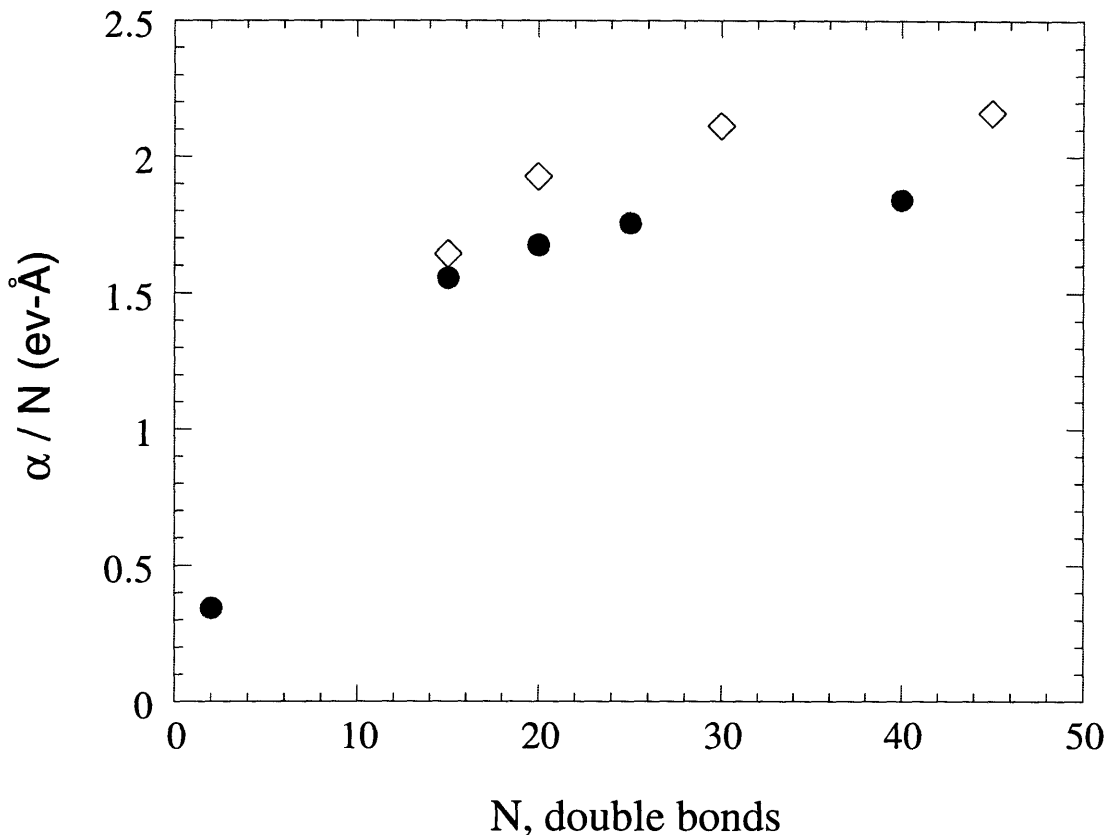
Figure 2-7: α/N from simulations (●) and theory (◇), $V_o = 0.026$ eV, $t_s = 2.15$ eV, $t_d = 2.85$ eV.

surements of the molecules used in the experiment, namely an error of factor of 2 [26]. The corrected experimental data are plotted in Figure 2-8. Also, note that there is an uncertainty in the value of the steric potential constant, V_o, used. We have used a value for V_o which may need to be modified for the particular molecules of the experiment.

We also study the absorption of long chains. We model the absorption of the $1^1A_g \rightarrow 1^1B_u$ electronic transition of a polyene of length ℓ, by

$$I_\ell(\omega) = \frac{\delta/\pi}{(\omega - \omega_\ell)^2 + \delta^2}\mu_\ell^2$$

where $\omega_\ell = A + B/\ell$ can be obtained by fitting experimental data in the usual way,

Figure 2-8: γ/N from simulations ($\square$), theory ($\diamond$) and experiment ($\bullet$).
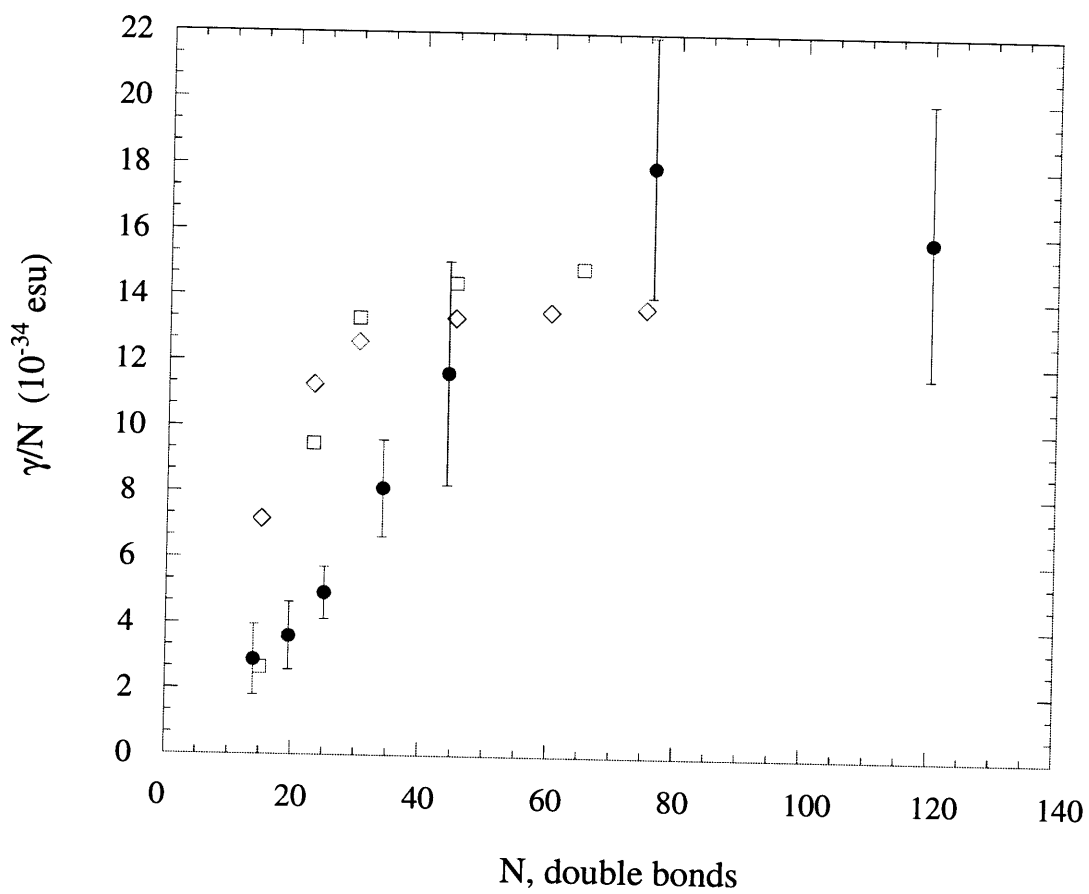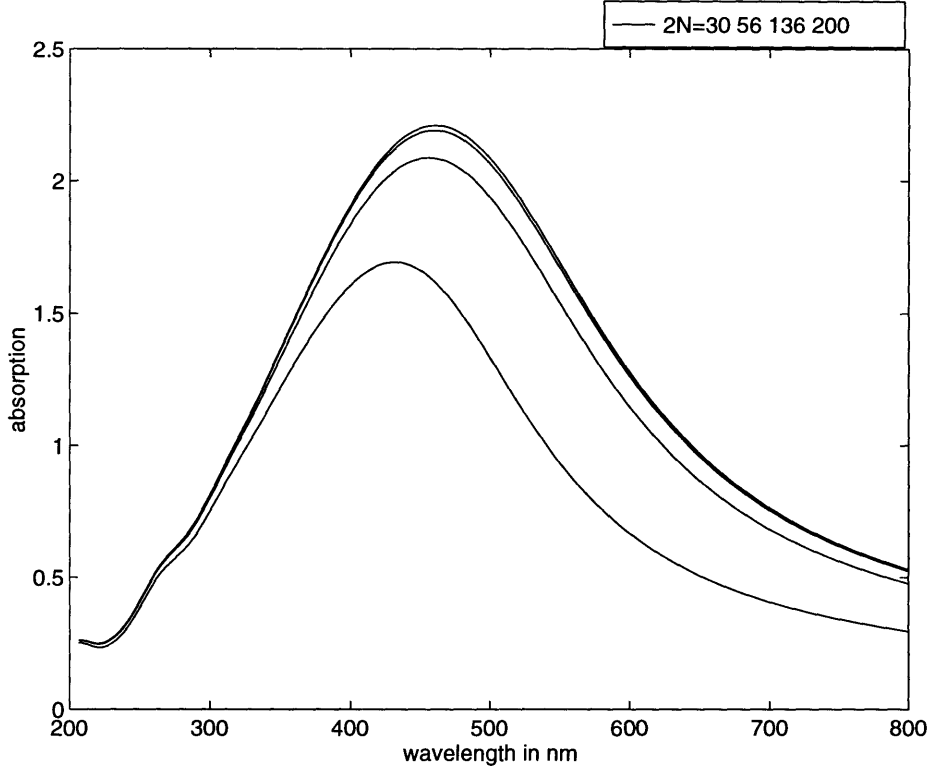
Figure 2-9: Absorption spectrum from theory.

and μ is obtained in the same manner as described in Section 2.4. So the absorption of a chain of N double bonds is given, according to our model by Eq. (2.8):

$$< I(\omega) > = \sum_{\ell} \frac{\delta/\pi}{\left(\omega - \omega_{\ell}\right)^2 + \delta^2} \mu_{\ell}^2 . \wp^N(\ell).$$

As in the case with γ, the agreement with experiment is closer after the corrected experimental data.

2.6 Discussion

Starting from a microscopic description, we propose an alternative way to consider conformational disorder on conjugated chains. Instead of focusing on the majority of small angular deviations of adjacent platelets, we consider the few big breaks or "flips". We propose that the distribution of the length of the segments between flips is the most relevant for the optical properties of these chains. Our predictions are supported by numerical simulations. Certain aspects of recent experimental observa-

42

tions are also accounted for. In the process, we derive the form of the phenomeno-logical term used to describe the conjugation effect of these systems and relate its parameters to measurable quantities, but retain the phenomenological form of the steric interactions. Describing steric interactions from a microscopic point of view would be a possible expansion of this work.

We notice in the calculations for γ (Figure 2-8), that the initial behavior of γ with the number of double bonds does not follow the experimental rate of change. This may be due to end effects, which are naturally more important in the smaller chains. A modified probability distribution of segment lengths to account for the end of the molecule may be more appropriate, and would explain the slow initial rise of the curves. Work in this direction is in progress.

In this work, we have not addressed at all the role of electron-electron interactions. We also did not consider the effect of bond length changes as conformation changes occur. The inclusion of those effects would give the possibility of studying their interplay and relative contributions of conformations to the electronic and optical properties of those systems.

Finally, recent experimental work [27] addresses the questions of scaling of the cubic nonlinearity in conjugated systems (poly-phenylene vinylene oligomers), and the role of conformational disorder emerges as an essential aspect in understanding the experiments.

Bibliography

[1] *Nonlinear Optical Properties of Organic Molecules and Crystals*, edited by D.S. Chemla and J. Zyss, (Academic Press, New York, 1987).

[2] *Conjugated Polymers*, edited by J.L. Brédas and R. Silbey, (Kluwer Academic Press, 1991).

[3] B. S. Hudson, B.E. Kohler, K. Shulten, in *Excited States* Vol.6 , edited by E.C. Lim, (Academic Press, 1982).

[4] A.J. Heeger, S. Kivelson, J. Schrieffer, W.P. Su, Rev. Mod. Phys **60**, 781 (1988).

[5] L. Salem, *The Molecular Orbital Theory of Conjugated Systems*, (W.A. Benjamin, New York, 1966).

[6] C. Cojan, G.P. Agrwal, C. Flytzanis, Phys. Rev. B **15**, 909 (1977).

[7] I.D.W. Samuel, I. Ledoux, C. Dhenaut, J. Zyss, H.H. Fox, R.R. Schrock, R.J. Silbey, Science **265**, 1070 (1994).

[8] R.H. Baughman and R.R. Chance, J. Chem. Phys. **47**, 4295 (1976).

[9] S.N. Yaliraki and R.J. Silbey, J. Chem. Phys., **104**, 1245 (1996).

[10] G. Rossi, R.R. Chance and R.J. Silbey, J. Chem. Phys. **90**, 7594 (1989).

[11] Z.G. Soos and K.S. Schweizer, Chem. Phys. Lett. **139**, 196 (1987).

[12] P.A. Pincus, G. Rossi, M.E. Gates, Europhys. Lett. **4**, 41 (1987).

[13] K.S. Schweizer, J. Chem. Phys., **85**, 4181 (1985); *ibid*, 1156 (1986); *ibid*, 1176 (1986).

[14] P. Garrin, J.P. Aimé, J.L. Fave, S. Ramakrishnan, G.L. Baker, Journ. de Phys. II **2**, 529 (1992).

[15] G. Rossi and A. Viallat, Phys. Rev. B **40**, 10036 (1989); G. Rossi and A. Viallat, J. Chem. Phys. **92**, 4548 (1990); A. Viallat, J. Chem. Phys. **92**, 4557 (1990).

[16] R. MacKenzie, J.M. Ginger, A.J. Epstein, Phys. Rev. B. **44**, 2362 (1991).

[17] J.L. Brédas, C. Quattrochi, J. Libent, A.C. MacDiarmid, J.M. Ginger, A.J. Epstein, Phys. Rev. B. **44**, 6002 (1991).

[18] B.E. Kohler and I.D.W. Samuel, J. Chem. Phys. **103**, 6248 (1995); B.E. Kohler and J.C. Woehl, J. Chem. Phys. **103**, 6253 (1995).

[19] W.P. Su, J.R. Schrieffer, A.S. Heeger, Phys. Rev. B **22**, 2099 (1980).

[20] J.R. Ackerman and B.E. Kohler, J. Chem. Phys., **80**, 45 (1984).

[21] N. Metropolis, A.W. Rosenbluth, M.N. Rosenbluth, A.H. Teller, E. Teller, J. Chem. Phys. **21**, 1087 (1953).

[22] I.D.W. Samuel *et al.*, in preparation.

[23] D.Yaron and R.J. Silbey, Phys. Rev. B **45**, 11655 (1992).

[24] S. Mukamel, A. Takahashi, H.X. Wang, G.H. Chen, Science **266**, 250 (1994).

[25] F.C. Spano and Z.G. Soos, J. Chem. Phys. **99**, 9265 (1993).

[26] R.R. Schrock, private communication.

[27] A. Mathy, K. Ueberhofen, R. Schenk, H. Gregorius, R. Garay, K. Müllen, C. Bubeck, Phys. Rev. B. **53**, 4367 (1996).

Chapter 3

Effects of an Applied Field on the Structure of Finite and Infinitely-long Polyene Systems

3.1 Introduction

Conjugated organic molecules and polymers have attracted attention for photonic applications due to their large nonlinear optical (NLO) responses. Optimization of those materials for building nonlinear optical devices has been the focus of recent research [1]. Central to the problem of optimization lies the question of the relation between structure, both chemical and geometric, to the electronic and optical properties, both linear and nonlinear. Understanding the relationship between geometric and electronic structure will enhance the optimization of design strategies.

In particular, donor-acceptor substituted polyenes have been suggested as an important class of organic molecules for their potential use in NLO devices [2]. It has been recently found by Marder *et al.* that, in small donor-acceptor polyenes, structure and optical responses (both linear and nonlinear) are connected in a simple way [3]. The π- electron bond order alternation (BOA) has been chosen as the parameter to describe the structure. Their idea is that the internal field of the molecule (due to

the donor-acceptor as well as the applied electric field) control its structure and hence the optical response. Numerical calculations support their conjecture [4]. To elucidate the origins of these results we study simple models which contain the essence of those physical systems and can be solved analytically. First, we compare the effect of the field on even and odd hydrocarbon chains. We consider the simplest possible cases, the three and four carbon linear polyenes and obtain exact functional forms between the field and displacement of atoms from equilibrium. We find those forms to differ, reflecting the different symmetries of the two systems. While the odd system's ground state energy contains odd power terms in field and displacement, the even one contains only even ones. We then proceed to find the effect of an applied field on the energy spectrum and structure of finite even membered carbon rings of any length. Within Hueckel theory, we find, that the presence of the field opposes the bond alternating structure. Finally, we examine a Hamiltonian, with the same spectrum as that of a polyene, and which can still be solved with the addition of an electric field. The electric field mimics the effect of the donor and acceptor on the π electrons. Here we focus on large systems and compare to effects seen numerically in small polyenes. We find that the presence of a field changes the states of a large 1-dimensional system dramatically. In order to ensure self-consistent solutions, in the large and weak field limit, the effective BOA parameter is forced to change with the electric field. This implies that this internal field may indeed drive the chemical and electronic structure, as already suggested, with important conclusions for the relations among polarizabilities as a function of the field.

In Section 3.2, we compare the ground state energy of odd and even chains in the presence of the field and reveal the complex behavior of the odd chains versus that of the even ones. In Section 3.3 we consider the effect of the applied field on even membered rings. We look at the stability of the bond alternating configuration in the presence of the field, through the second derivative of the ground state, similar in spirit to the calculation of Longuet-Higgins and Salem [5]. We find that the field favors the bond alternating chain, and that the critical length where this configuration becomes the stable one, decreases with the field. In Section 3.4 we introduce the

47

model system, namely a site alternating chain model or equivalently a two coupled band model. In the absence of field, we make the connection to the polyenes and we proceed in Section 3.5 to study the effect of a constant electric field on the donor-acceptor substituted chain. In particular, we investigate the relationship of the bond order alternation with this internal field. We choose this property as most relevant to the study of the connection between structure and optical properties. Indeed we show that the field drives the chemical structure through BOA. The implications of this are discussed in Section 3.6.

3.2   Odd vs even polyenes in presence of an applied field

In this section, we begin by considering the simplest case, 3 and 4 carbon open chain molecules, and we obtain the ground state energy as a function of the bond alternation parameter, x, defined below, and the applied field, f. We are interested in how the applied field influences the structure of those systems. We find that the functional dependence is quite different, reflecting the different symmetries of the two systems. In particular, while the properties of the even system contain only even powers in f and x, those of the odd also contains odd power terms, such as xf. We will show in Section 3.3 that the former result persists for the even rings of any length.

We denote the resonance integrals across the double (β_2) and single (β_1) bonds by

$$\beta_2 \leq \beta_1 < 0. \tag{3.1}$$

We express alternately increasing and decreasing bond lengths by modifying the resonance integrals, so that

$$\beta_1 = \beta_0 e^{-x}, \qquad \beta_2 = \beta_0 e^{x} \tag{3.2}$$

where x is a small positive quantity (β_0 is negative).

In particular, for the radical, in site representation where the charge of an electron,

48

$e = 1$, and f is the applied field

$$\begin{pmatrix} f & \beta_0 e^{-x} & 0 \\ \beta_0 e^{-x} & 0 & \beta_0 e^{x} \\ 0 & \beta_0 e^{x} & -f \end{pmatrix}$$

For $x = 0$, in terms of $y = f/\beta_0$ the three orbital energies are

$$\lambda^0 = 0 \qquad \lambda_{\pm}^0 = \pm\sqrt{y^2 + 2}$$

The first order corrections in x are

$$\epsilon_{\pm} = \frac{-2yx}{(y^2 + 2)}.$$

$$\epsilon_0 = \frac{4yx}{(y^2 + 2)}$$

On the other hand, for the four membered chain, no term linear in f appears:

$$\begin{pmatrix} 2f & \beta_0 e^{-x} & 0 & 0 \\ \beta_0 e^{-x} & f & \beta_0 e^{x} & 0 \\ 0 & \beta_0 e^{x} & -f & \beta_0 e^{-x} \\ 0 & 0 & \beta_0 e^{-x} & 2f \end{pmatrix}$$

The orbital energies are now (again in terms of $y = f/\beta_0$)

$$\epsilon_{1,2} = \pm 1/2\sqrt{10y^2 + 4\cosh 2x + 2e^{-2x} + 2S}$$

$$\epsilon_{3,4} = \pm 1/2\sqrt{10y^2 + 4\cosh 2x - 2e^{-2x} + 2S}$$

where $S = \sqrt{9y^4 + e^{4x} - 12\sinh 2x + 30y^2 e^{-2x} + 4}$

The xf (or xy) terms are also absent for the 6 membered chain. The differences become apparent, when we look at the ground state energy as a function of the BOA parameter x for different fields (Figure 3-1). We believe this difference in behavior to

49

persist for longer chains, and is due to the inherent ground state degeneracy of the odd open chains (which is absent in the even chains).

Let us consider the 3 carbon open chain further. To mimic a donor-acceptor substituted polyene, we replace f by $g = -\Delta + f$ in the Hamiltonian matrix. Thus at zero applied field, site 1 has energy $-\Delta$ and site 3 energy $+\Delta$. In the presence of the field f, the site energies are transformed to $+g\,(-\Delta + f)$ and $-g$, respectively. Note that the energies retain the same form, with f replaced by g so that g is the effective field on the system (the sum of the applied field f and the molecular field s).

Now consider a 3 electron, 3 carbon chain. The total π energy in the Hueckel model is then

$$E^{\pi}(x, f)/\beta_0 = 2\epsilon_+ + \epsilon_0 = +2\sqrt{y^2 + 2} + \mathcal{O}(g^2 x^2)$$

where $y = g/\beta_0$. We can also compute the dipole moment of this system to this order and find (as a function of field)

$$
\begin{aligned}
\mu(x; f) &= 2\left[\frac{-y}{(y^2 + 2)^{1/2}} + \frac{2x(2 - y^2)}{(y^2 + 2)^2} \right] + \frac{4x(y^2 - 2)}{(y^2 + 2)^2} \\
&= \frac{-2y}{(y^2 + 2)^2} + \mathcal{O}(g^2 x^2) = -(\frac{\partial E^{\pi}}{\partial y})_x.
\end{aligned}
$$

Thus μ is an even function of x for small x.

If we now consider a 2 electron, 3 carbon chain, the total energy and dipole moment become

$$E^{\pi}(x, f)/\beta_0 = 2\epsilon_+ = +2\sqrt{y^2 + 2} - \frac{4xy}{(y^2 + 2)}$$

and

$$\mu(x; f) = \frac{-2y}{(y^2 + 2)^{1/2}} - \frac{4x(y^2 - 2)}{(y^2 + 2)^2}.$$

The σ electron energy is given by

$$E^{\sigma}(x, f) \approx 1/2\omega^2 x^2,$$

50

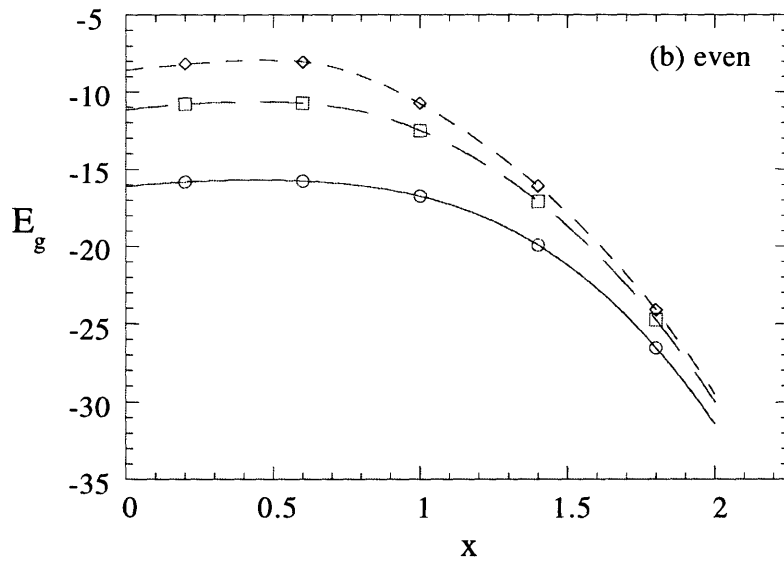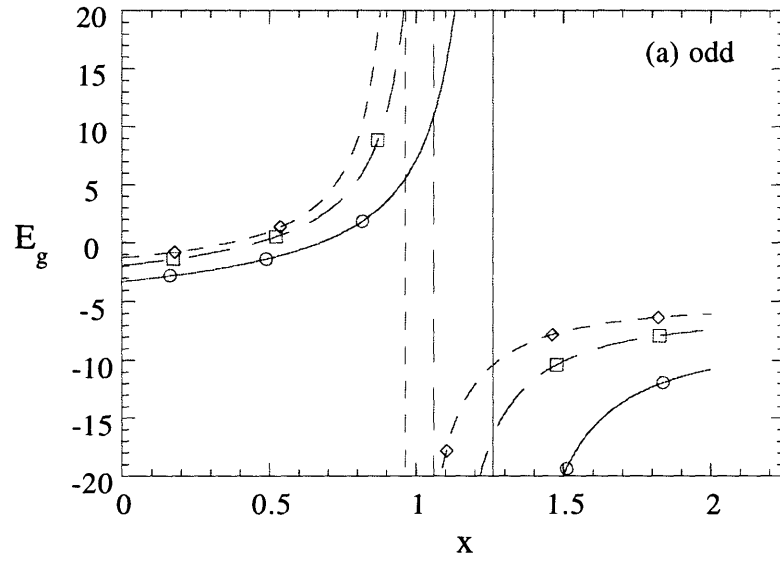Figure 3-1: The ground state energy E_g of the (a) odd and (b) even system as a function of the BOA parameter x for different values of f/β_0 : $(*).0145(\circ).50(x)1.0(+)1.45$.

so that the equilibriumm value of x as a function of field is given by

$$x_{eq} = \frac{4y}{\omega(y^2 + 2)} = \frac{4(f - \Delta)/(\beta_0 \omega)}{(f - \Delta)^2 + 2}. \tag{3.3}$$

Thus for $|f - \Delta| \le \sqrt{2}$, the bond alternation, x_{eq}, is a linear function of applied field, and is zero at $f = \Delta$. This is similar to the relationship found in Ref. [3]. Moreover, x_{eq} saturates as a function of y and then goes to zero again for large y. In the intermediate range, however, x_{eq} has a slightly sigmoidal shape as a function of field (see Figure 1 of Ref. [4]). We now calculate the molecular polarizabilities as a function of field, by differentiating E^π with respect to y. Note that x_{eq} is given by Eq. 3.3, so that, for practical purposes, in the region $|y| < \sqrt{2}$, y is proportional to x_{eq}. Thus the molecular polarizabilities α, β and γ have the forms found in Ref. [3] and [4] (see Figure 7 of Ref. [4]) as a function of x_{eq} (optimized in the field).

By examining any odd atom donor acceptor system, we find the same qualitative behavior as above. The molecules considered in Ref. [4] are 11 atom sustems, with (effectively) 10 π electrons.

We see from this analysis that the qualitative results of Ref. [3] and [4] are present already in the Hueckel model of π electron molecules.

3.3 Bond alternation in finite cyclic polyenes in presence of an applied field

In this section, we consider the effect of a weak electric field on the ground state energy and bond alternation of even polyene rings of the form, $C_{4n+2}H_{4n+2}$. Here, we consider finite systems of any length. Also, we make unambiguous use of the periodic boundary conditions by considering rings, with the appropriate form of the dipole moment operator, as we show later. We express the ground state energy in terms of the displacement of the carbon atoms from the equal bond length configuration, and the applied field. The calculation proceeds in the spirit of that of that of Longuet-Higgins and Salem [5] (LHS): the σ bond energy as a function of x is given by $1/2\omega^2 x^2$,

favoring equal bond lengths ($x = 0$); the π contribution is given by

$$E_g^\pi(x, f) = E^\pi(x, 0) - \frac{1}{2}\alpha(x)f^2 \qquad (3.4)$$

where f is the applied field, x is the bond order alternation parameter and $\alpha(x)$ is the polarizability as a function of x. LHS [5] found that $(\frac{d^2 E_g^\pi}{dx^2}(x, 0))_{x=0}$ was negative and so the π energy favored bond alternation (i.e. $x \neq 0$). The question we ask is whether the field dependent term in 3.4 favors $x = 0$ (i.e. $(d^2\alpha/dx^2)_{x=0} < 0$) or $x \neq 0$ (i.e. $(d^2\alpha/dx^2)_{x=0} > 0$). As in LHS, the ground state energy is taken to be the sum of the occupied orbitals (for a ring of $4N + 2$ atoms)

$$E_g^\pi(x, 0) = 2 \sum_{j=-N}^{N} \epsilon_j$$

where

$$\epsilon_j = \sqrt{\beta_1^2 + \beta_2^2 + 2\beta_1\beta_2 \cos[2j\pi/(2N + 1)]} \qquad (3.5)$$

β_1 and β_2 are the resonance integrals of the single and double bonds as defined in Eq. 3.1 and 3.2. The actual change in bond length is equal to ax where $a = .31\mathring{A}$ in [5]. The second derivative of $E_g^\pi(x, 0)$ with respect to x was found [5] to be negative and increase as $n \ln n$.

To see the effect of the field on the energy as a function of x, we now proceed to calculate the second derivative of the linear polarizability with respect to x. The standard expression from perturbation theory for α

$$\alpha = 2\sum_{n}' \frac{| < \psi_g(x)|\mu|\psi_e(x) > |^2}{E_e(x) - E_g(x)} \qquad (3.6)$$

where $< \psi_g(x)|\mu|\psi_e(x) >$ is the transition moment matrix element between an excited and the ground state. The prime denotes a restricted sum, due to exclusion of the ground state. For consistent use of periodic boundary conditions in finite systems, the periodic representation of the dipole moment operator is the appropriate one [6].

53

For a ring of $4N + 2$ carbon atoms,

$$
\begin{aligned}
\hat{\mu} &= \frac{e(2N+1)l}{2\pi} \left[\sum_{j=-n}^{n} \{ \cos(\frac{2\pi j}{2N+1} + x_1) |2j\rangle\langle 2j| \right. \\
&+ \left. \cos(\frac{2\pi(j+1/2)}{2N+1} + x_2) |2j+1\rangle\langle 2j+1| \} \right]
\end{aligned} \tag{3.7}
$$

where $l = 2l_0$ is twice the equal bond length magnitude, and x_1, x_2 are angles defined in such a way that the single and double bond lengths are given for small x by

$$
l_s = l_0 + ax
$$

and

$$
l_d = l_0 - ax.
$$

We find

$$
x_1 = -x_2 = \frac{ax2\pi}{(2N+1)l}.
$$

Since the HOMO to LUMO transition carries most of the oscillator strength, we consider only this excitation in the sum. α now becomes

$$
\alpha(x) \simeq 2\frac{|\langle\psi_{\text{HOMO}}|\hat{\mu}|\psi_{\text{LUMO}}\rangle|^2}{\Delta E}. \tag{3.8}
$$

The appropriate wavefunctions are now those for $j = N$

$$
\psi_{\text{HOMO}} = \frac{1}{\sqrt{4N+2}} \sum_{j} \{ e^{ij\theta_N - i\gamma_N} |2j\rangle + e^{i(2j+1)\theta_N/2 + i\gamma_N} |2j+1\rangle \}. \tag{3.9}
$$

where,

$$
\theta_N = \frac{2\pi N}{2N+1} \simeq \pi
$$

and

$$
\gamma_{\text{HOMO}}(x) = 1/2 \arctan(\tanh x \tan \frac{\pi N}{2N+1}) = -\gamma_{\text{LUMO}}(x).
$$

From Eq. 3.5, we obtain for the energy difference,

$$\Delta E = 2|\beta_0|\sqrt{2\cosh 2x + 2\cos \frac{2N\pi}{2N+1}} \tag{3.10}$$

Substituting Eqs. 3.7,3.9 and 3.10 into Eq. 3.8, for a small displacement of bonds x,

$$\alpha(x) = \frac{e^2 l^2 (2N+1)}{8\pi^2 |\beta_0| \sqrt{2\cosh 2x + 2\cos \frac{2N\pi}{2N+1}}} \times$$

$$\left| \left[\sum_j \cos(\frac{2\pi j}{2N+1} + x_1(x)) e^{-2\pi j/2N+1} \right. \right.$$

$$\left. \left. - \sum_j \cos(\frac{2\pi(j+1/2)}{2N+1} + x_2(x)) e^{2\pi(j-1)/2N+1} \right] \right|^2 \tag{3.11}$$

The sums in Eq. 3.11 can be done and we find

$$\alpha(x) = \frac{e^2 a^2 x^2/(2N+1)}{8|\beta_0|[x^2 + \frac{\pi^2}{(2N+1)^2}]^{1/2}}. \tag{3.12}$$

Therefore $[\alpha'']_{x=0} > 0$, and

$$E_g^\pi(x, f) = E_g^\pi(x, 0) - \frac{1}{2}(\alpha(0) + [\alpha''(x)]_{x=0}x^2)f^2 \tag{3.13}$$

so that the external field works in the same direction as the $\pi-$electron energy; that is to favor bond alternation.

3.4   Infinitely-long chains: Description of the model systems

We now treat infinitely long chains. We briefly introduce the Hamiltonian of the conjugated polyenes, as well as its spectrum in the absence of electric field. We then describe the two-coupled band model we have chosen to emulate the behavior of polyenes. The effect of the donor and acceptor at the ends of the chain on the π electrons is mimicked by a constant electric field across the direction of the chain.

In the absence of field (no donor-acceptor) we show that this model has the same spectrum as the unsubstituted polyene. In this work, we consider systems of large N. Since previous work looked at small molecules, it is interesting to investigate whether ideas of the connection between BOA and field still prevail at the large N limit.

3.4.1 Polyenes

Polyenes of $2N$ carbon atoms have been extensively and successfully modeled as one dimensional systems of $2N$ sites, each occupied by an atom with one unpaired electron [7, 8]. Bond dimerization is imposed here although the electron-phonon coupling interaction is explicitly neglected.

The Hamiltonian

$$
\begin{aligned}
H = \quad & - \sum_\sigma \sum_{\ell=1}^{N} [t_d a^\dagger_{\ell\sigma,1} a_{\ell\sigma,2} + t_s a^\dagger_{\ell\sigma,2} a_{\ell+1\sigma,1} + \text{h.c.}] \\
& + \sum_\sigma \sum_{\ell,i} eEd\ell a^\dagger_{\ell\sigma,i} a_{\ell\sigma,i}
\end{aligned}
\tag{3.14}
$$

describes the hoping of π electrons along the chain with transfer integrals t_s and t_d along single and double bonds respectively as well as the site energies of the states in the presence of a static electric field. $a^\dagger_{\ell\sigma,i}(a_{\ell\sigma,i})$ creates(destroys) an electron with spin σ on the ith position of the ℓth unit cell and obeys fermi statistics. Each of the N unit cells, ℓ, contains two carbon atoms on sites $i = 1, 2$ - a double and a single bond of fixed length respectively. Also, in Eq. (3.14), e is the electron charge, F the applied electric field in units of $eV/\mathring{A}$ and d the unit cell distance in $\mathring{A}$. We adopt the following definition throughout the chapter for simplification of notation: $\tilde{f} \equiv eFd$.

Consider the zero field case (i.e. polyene without donor-acceptor groups.) With the help of Fourier transforms of the a_ℓ's, invoking periodic boundary conditions:

$$
a_{k\sigma,i} = \frac{1}{\sqrt{N}} \sum_\ell e^{-ik\ell} a_{\ell\sigma,i} \quad \text{with} \quad k = 2\pi j/N, \quad j = 0, 1, .., (N-1)
$$

56

we diagonalize the Hamiltonian, with eigenvalues

$$\epsilon_k = \pm \left[t_s^2 + t_d^2 + 2t_s t_d \cos k \right]^{1/2}. \tag{3.15}$$

In the absence of electric field we obtain then the conduction and valence bands with an energy gap $E_g = 2|(t_s - t_d)|$ at $k = \pi$.

3.4.2 Two coupled bands

To mimic the behavior of the conjugated polyenes we look for a model which exhibits an energy spectrum of the form of Eq. 3.15 and which can be solved analytically in the presence of a field. We consider the site alternating chain model with single transfer matrix element, as one close in spirit to the bond-alternated chain. In this section, we will first show that this model is equivalent to a two band model with interband interaction. Then, we will establish the connection with the bond alternated spectrum in the absence of field, (i.e. of the polyenes) through the parameters of the Hamiltonian described below. In the presence of the effective field, which models the donor-acceptor substituted systems, they become effective parameters.

The site alternating chain Hamiltonian in the presence of a field is

$$
\begin{aligned}
H &= \sum \Delta (-1)^\ell b_\ell^\dagger b_\ell + t \sum [b_\ell^\dagger b_{\ell+1} + \text{h.c.}] \\
&+ \sum_\ell \tilde{f} \ell b_\ell^\dagger b_\ell.
\end{aligned} \tag{3.16}
$$

In this Hamiltonian, Δ, t, and $\tilde{f}$ are parameters to be chosen. If we define the even sites with $+\Delta$ by $a_{\ell,1}$ and the odd sites with $-\Delta$ by $a_{\ell,2}$, then there are two sites in the unit cell labelled 1 and 2, similar to the polyene case in Eq. (3.14). With

$$a_{\ell,1} = b_\ell, \quad \ell \quad \text{even}$$
$$a_{\ell,2} = b_\ell, \quad \ell \quad \text{odd}$$

in the zero field case, the Hamiltonian then becomes

$$H_o = - \Delta \sum_{\ell} [a_{\ell,1}^{\dagger} a_{\ell,1} - a_{\ell,2}^{\dagger} a_{\ell,2}] + t \sum [a_{\ell,1}^{\dagger} a_{\ell,2} + \text{h.c.}]$$
$$+ t \sum [a_{\ell,2}^{\dagger} a_{\ell+1,,1} + \text{h.c.}]. \tag{3.17}$$

The eigenvalues of H_o can be found by defining

$$a_{k,i} = \frac{1}{\sqrt{N}} \sum_{\ell} e^{-ik\ell} a_{\ell,i}$$

so that

$$H_o = \Delta \sum_{k} [a_{k,1}^{\dagger} a_{k,1} - a_{k,2}^{\dagger} a_{k,2}] + t \sum [(1 + e^{ik}) a_{k,1}^{\dagger} a_{k,2} + \text{h.c.}].$$

This Hamiltonian is then broken into 2×2 blocks with eigenvalues

$$\epsilon_k = \pm \left[\Delta^2 + t^2 (2 + 2\cos k) \right]^{1/2}. \tag{3.18}$$

If we compare to the bond order alternated polymer eigenvalues in Eq. (3.15) we see
that they coincide if we make the substitutions

$$t^2 = t_s t_d \qquad \Delta^2 = (t_s - t_d)^2 \tag{3.19}$$

After making the identifications of our model system to the polyenes of interest we
proceed to study their behavior in the presence of electric field. The solutions for a one
band Hamiltonian with a constant transfer integral have been studied in the context
of crystals in uniform electric fields [9, 10] and recently in that of semiconductor
superlattices [11]. They are referred to in the literature as the Wannier-Stark Ladder
eigenstates. The solutions for the simplest case are given in Appendix A.

3.5 Two coupled bands: solutions in the presence of a constant electric field

In this section we consider the effect of the molecular effective electric field or equivalently the donor-acceptor in the chain system described in Section 3.4.2. Using the procedure outlined in Appendix A we show the dramatic change of the eigenvalues and eigenfunctions in the presence of field. In particular, we find that, in order to obtain a self-consistent solution, it is necessary to vary the effective parameters $\Delta^2 = (t_s - t_d)^2$ and $t^2 = t_s t_d$ as a function of the electric field. This implies that there exists a correlation of the BOA with the effective field.

Rewriting the Hamiltonian (3.16) we have

$$H = \sum [(-1)^\ell \Delta + \ell \tilde{f}] b_\ell^\dagger b_\ell + t \sum [b_\ell^\dagger b_{\ell+1} + \text{h.c.}]. \tag{3.20}$$

To diagonalize this Hamiltonian we introduce the transformation

$$b_\ell = (-1)^\ell \sum_n J_{\ell-n}(2t/\tilde{f}) c_n$$

leading to

$$
\begin{aligned}
H &= \sum_{\ell,n,n'} [(-1)^\ell \Delta + \ell \tilde{f}] J_{\ell-n}(2t/\tilde{f}) J_{\ell-n'}(2t/\tilde{f}) c_n^\dagger c_n' \\
&\quad - t \sum_{\ell,n,n'} [J_{\ell-n}(2t/\tilde{f}) J_{\ell+1-n'}(2t/\tilde{f}) c_n^\dagger c_{n'} + \text{h.c.}]. \tag{3.21}
\end{aligned}
$$

Using the Bessel function equalities, we find

$$H = \sum_n n\tilde{f} c_n^\dagger c_n + \Delta \sum_{n,n'} (-1)^n J_{n-n'}(2t/\tilde{f}) c_n^\dagger c_{n'}.$$

Now, introduce the Fourier transforms of the c_n's:

$$c_k = \frac{1}{\sqrt{N}} \sum_n e^{ikn} c_n, \quad \text{and} \quad \frac{dc_k}{dk} = \frac{i}{\sqrt{N}} \sum_n n c_n e^{ikn}$$

59

to find

$$H = \sum_k \mathcal{H}_k$$

with

$$\mathcal{H}_k = -(c_k^\dagger, c_{k+\pi}^\dagger) \begin{pmatrix} i\tilde{f}\frac{d}{dk} & 2\Delta e^{-i2\alpha \sin k} \\ 2\Delta e^{i2\alpha \sin k} & i\tilde{f}\frac{d}{dk} \end{pmatrix} \begin{pmatrix} c_k \\ c_{k+\pi} \end{pmatrix}$$

and $\alpha = 2t/\tilde{f}$. To solve for the eigenfunctions and eigenvalues for a particular k, we write

$$\psi_k = \tilde{A}_k c_k^\dagger |0\rangle + \tilde{B}_k c_{k+\pi}^\dagger |0\rangle$$

so that

$$(\epsilon - i\tilde{f}\frac{d}{dk})\tilde{A}_k = 2\Delta e^{-i2\alpha \sin k} \tilde{B}_k$$

$$(\epsilon - i\tilde{f}\frac{d}{dk})\tilde{B}_k = 2\Delta e^{i2\alpha \sin k} \tilde{A}_k \qquad (3.22)$$

Defining

$$A_k = \tilde{A}_k e^{-i\epsilon k/\tilde{f}} \qquad B_k = \tilde{B}_k e^{-i\epsilon k/\tilde{f}} \qquad (3.23)$$

we find that the A_k and B_k obey the second order differential equation:

$$A_k'' + (\frac{2\Delta}{\tilde{f}})^2 A_k + i2\alpha \cos k A_k' = 0$$

$$B_k'' + (\frac{2\Delta}{\tilde{f}})^2 B_k - i2\alpha \cos k B_k' = 0 \qquad (3.24)$$

where the prime means differentiation with respect to k. The form of this equation is reminiscent of that of the Mathieu equation. We will make use of this in the weak field ($\alpha \gg 1$) and strong field ($\alpha \ll 1$) limits. To capitalize on this resemblance, we define

$$\tilde{k} = k - \pi/2 \quad \text{and} \quad A_k = e^{i\alpha \cos \tilde{k}} u_A(\tilde{k}) \quad B_k = e^{-i\alpha \cos \tilde{k}} u_B(\tilde{k}) \qquad (3.25)$$

60

and find for $u \equiv u_A(\tilde{k})$

$$u'' + [(\frac{2\Delta}{\tilde{f}})^2 + \frac{\alpha^2}{2} - i\alpha\cos\tilde{k} - \frac{1}{2}\alpha^2\cos(2\tilde{k})]u = 0. \qquad (3.26)$$

In the high field limit ($\alpha \ll 1$), we can neglect the α^2 term; in the low field limit ($\alpha \gg 1$) we can neglect the α term with respect to the α^2 term. In both cases, we can bring the equation into the form of the Mathieu equation:

$$u'' + [a - 2q\cos(2\tilde{k})]u = 0.$$

However, the values of a and q are different in the two limits.

On one hand, in the low field case, we have

$$u'' + [(\frac{2\Delta}{\tilde{f}})^2 + \frac{\alpha^2}{2} - \frac{\alpha^2}{2}\cos(2\tilde{k})]u = 0 \qquad (3.27)$$

so that ,

$$a = (\frac{2\Delta}{\tilde{f}})^2 + \frac{\alpha^2}{2}, \qquad q = \frac{\alpha^2}{4}$$

and since $\alpha = 2t/\tilde{f}$,

$$\frac{a}{q} = 2 + 4\frac{\Delta^2}{t^2}$$

is independent of the field.

From the definition of Δ and t used to connect this model to that of an alternating polyene (Eq. 3.19), we find

$$\frac{\Delta^2}{t^2} = \frac{(t_s - t_d)^2}{t_s t_d}$$

so that

$$\frac{a}{2q} = 1 + 2\frac{(t_s - t_d)^2}{t_s t_d}$$

is a measure of the bond alternation (or $t_s - t_d$).

In the high field limit, we neglect the α^2 terms in Eq. 4.12 to find

$$u'' + [-i\alpha \cos 2\,\tilde{\tilde{k}}]u = 0. \qquad (3.28)$$

Here,

$$a = 0, \quad q \equiv is = \frac{i\alpha}{2} = \frac{it}{\tilde{f}}, \quad \tilde{\tilde{k}} = \tilde{k}/2 \qquad (3.29)$$

We have also neglected $(\frac{2\Delta}{\tilde{f}})^2 \ll 1$, since Δ is of the same order of magnitude as t. We focus our attention on the ratio a/q because the particular form of the Mathieu equation solutions depends upon the values of (a, q). Details of the Mathieu solutions pertinent to our discussion are given in Appendix B.

Before we proceed we note that it is the weak field regime that is relevant for the study of polyene molecules. Since t is of the order of ev and $\tilde{f}$ of the order of 10^{-1} eV, $\alpha \gg 1$. The numerical values of the parameters are such that the high field regime corresponds to an unphysical region for donor-acceptor substituted polyenes. Rather, it is appropriate for the semiconductor superlattices, quasi one-dimensional structures with periods of 100 Å [12].

We concentrate now on the low field regime, since it is the physically relevant one. From the condition that the $\tilde{A}_k$ satisfy, namely that $\tilde{A}_k = \tilde{A}_{k+2\pi}$, we find, by using Eq. 3.23 and 3.25, that $u(\tilde{k})$ have to obey the following equation

$$\exp(i2\pi \frac{\epsilon}{f}) = [\frac{u(\tilde{k})}{u(\tilde{k} + 2\pi)}]$$

so that for the ladder spectrum (ϵ/f integer) we obtain

$$\tilde{u}_k = \tilde{u}_{k+2\pi} \qquad (3.30)$$

Now, for (a, q) real, the Mathieu equation has solutions with period 2π. Most importantly, these solutions are special in that they define the "characteristic curves" which divide the plane of Mathieu solutions into regions of stability and instability [13]. This implies that there exists a functional dependence between a and q,

namely the family of curves $a = a_{2n+1}(q)$ and $a = b_{2n+1}(q)$ are obtained. This implies then the functional dependence of Δ and $\tilde{f}$. The first few curves may be seen in Figure 3-2. We have already identified $\Delta = |t_s - t_d|$ to the difference of electron transfer across single and double bonds. As such it is related to the bond order alternation: $\Delta = 0$ corresponds to the equal bond length situation, where the $BOA = 0$; at the other extreme, the maximum value of Δ corresponds to the chain of maximum dimerization where the BOA is maximum. We express everything in units of t, a system dependent parameter. So we seek the relationship between Δ/t and $\tilde{f}/t$ in the limiting cases of low and high field. Since Δ/t is a constant for each system in our Hamiltonian formulation, its value is not altered by changing the effective field. Nevertheless, the 'phase diagram' of Δ/t versus $\tilde{f}/t$ obtained from the relation of those parameters to those of the Mathieu equation, yields indirect information on the effect of the effective field on the BOA. In such a diagram, each system will fall and follow a different curve depending on the value and t.

Finally, we notice is that, in the high field case, one of the Mathieu parameters is imaginary, $q = is$. We thus expect the $(a, |q|)$ stability "landscape" to differ from the one for real (a, q). The behavior of the new characteristic curves, which define the regions of stability, have already been numerically obtained for imaginary q [15]. Here, a and q are independent of Δ in the high field regime, i.e. the field has no longer any effect on the BOA.

3.6 Conclusions

In this work, we have investigated the effect of an applied electric field on the energy spectrum and the structure of polyene systems. Changes in structure have been studied through the bond order alternation, or the extent of the difference between single and double bonds across the conjugated chain. Our work was motivated by recent conjectures that the BOA plays an important role in determining the nonlinear optical response, in conjugated molecules with strong electron donor and acceptor substituents [4], where the applied field was intended to mimic the effect of the donor-
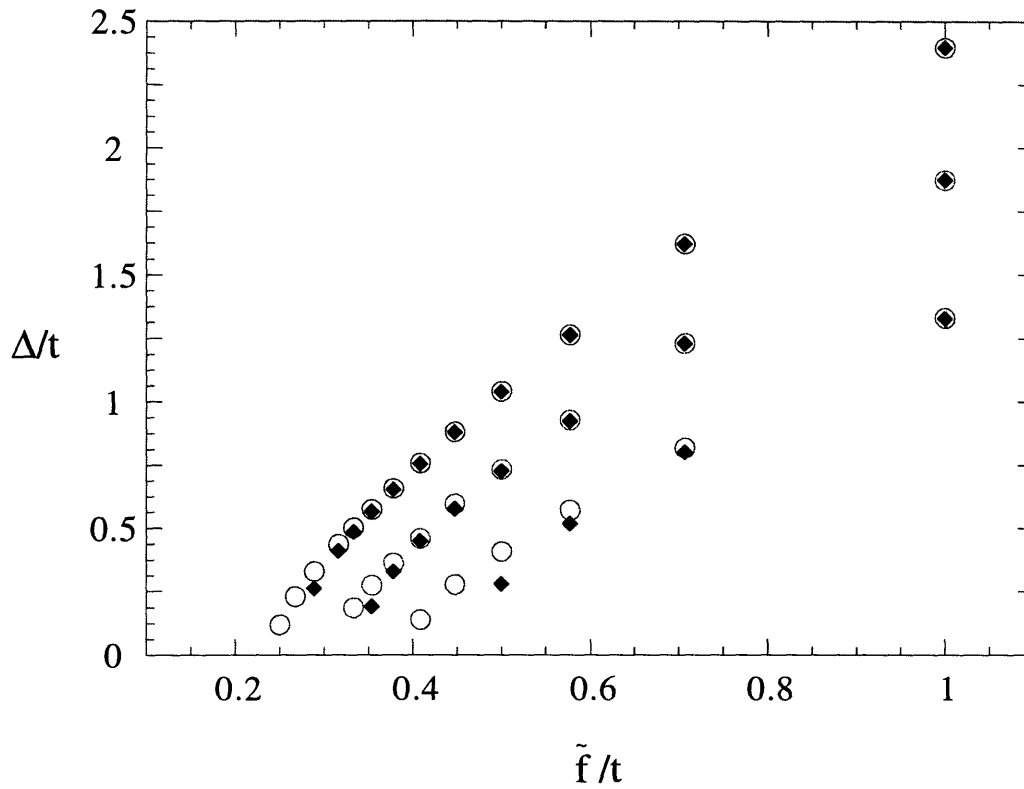
Figure 3-2: The BOA parameter as a function of applied field, $\tilde{f}/t$, from the odd characteristic mathieu curves: the (○) come from the a curves and the (◇) from the b. Here, the results from $a_3, b_3, a_4, b_4, a_5, b_5$ are depicted. The numerical values are from Ref. [13].

acceptor groups as well as the surrounding medium. We compared the functional form of the energy as a function of the field and and BOA in even and odd chains, by studying the smallest possible systems and found a striking difference between the two. Following Longuet-Higgins and Salem [5], we found that the field dependent term in the second derivative of the ground state energy enhances the bond alternation effect; that is, it acts in the same direction as the π electron energy term calculated by LHS. Finally, we considered large systems, where the effect of the field produces the ladder spectrum, and found that the BOA and the field are interdependent.

In all cases, the bond alternating chain was favored by the presence of the field. The equal bond length chain was not observed in the weak field limit, where all our calculations have been done. This result agrees with the findings of Ref. [16]. Although the effect of the applied field is profound, the specific forms needed to control the NLO properties were not recovered as suggested [4], similarly to the findings of others [16, 17], except in the case of odd atom donor-acceptor radicals.

3.7 Appendix A: The Wannier-Stark ladder Hamiltonian

The simplest -single band- case is treated here in the presence of a static electric field to illustrate the Wannier Stark eigenstates and their corresponding eigenvalues. A chain of N sites ($\lim N \to \infty$) at constant lattice spacing, d, (i.e. equal bond lengths) within the tight binding approximation with nearest-neighbor transfer integral, t, is considered. The Hamiltonian is then

$$H = \sum_{\ell=-N/2}^{N/2} t[a_\ell^\dagger a_{\ell+1} + \text{h.c}] + \sum_{\ell=-N/2}^{N/2} \tilde{f}\ell a_\ell^\dagger a_\ell, \qquad (3.31)$$

where $a_\ell^\dagger(a_\ell)$ is the creation (annihilation) operator at the ℓth site. The solutions of the eigenvalue equation $H\Psi = E\Psi$ for Eq. (3.31) obey the following equation:

$$\ell \tilde{f} c_\ell + t(c_{\ell+1} + c_{\ell-1}) = \epsilon c_\ell \qquad (3.32)$$

where c_ℓ is the expansion coefficient of Ψ in terms of localized Wannier states,i.e. we have used

$$\Psi = \sum_{\ell=-N/2}^{N/2} c_\ell a_\ell^\dagger |0\rangle$$

to obtain Eq. (3.32) from Eq. (3.31). Eq. (3.32) has the same form as the recursion relation obeyed by the Bessel functions. More specifically the general solution of the recursion relation:

$$f_{\nu+1}(z) + f_{\nu-1}(z) = (2\nu/z)f_\nu(z)$$

is [18]

$$f_\nu = AJ_\nu(z) + BY_\nu(z), \tag{3.33}$$

where $J_\nu(z)$ and and $Y_\nu(z)$ are the Bessel functions of the first and second kind respectively of order ν and argument z. A and B are constants. But, since $Y_\nu(z) \to \infty$ as $z \to \infty$, B is set to zero to ensure well behaved eigenfunctions. Similarly, if ν is not an integer the J_ν diverge [18]. Hence, the appropriate coefficients are

$$c_\ell = AJ_{\ell-n}(2t/\tilde{f}) \equiv c_\ell^n \qquad n = \epsilon/(\tilde{f}) = \text{integer}. \tag{3.34}$$

In this case it turns out that the eigenfunctions are orthonormal as it follows from two of the Bessel function identities [18]:

$$\sum_{\ell=-\infty}^{\infty} J_\ell^2(z) = 1, \tag{3.35}$$

and

$$\sum_{\ell=-\infty}^{\infty} J_{\ell+n}(z)J_{\ell+n'}(z) = \delta_{n,n'}. \tag{3.36}$$

Finally, the Wannier-Stark eigenstates,ψ_n, are

$$\begin{aligned} c_n^\dagger |0\rangle \equiv |n\rangle &= \sum_\ell J_{\ell-n}(2t/\tilde{f})a_\ell^\dagger |0\rangle \\ &\equiv \sum_\ell J_{\ell-n}(2t/\tilde{f}) |\ell\rangle \end{aligned} \tag{3.37}$$

66

with eigenvalues

$$\epsilon_n = n\tilde{f}. \tag{3.38}$$

This equidistant level quantization gives rise to the name of Stark Ladder used in the literature to refer to this type of Hamiltonian.

3.7.1 Properties of Wannier Stark eigenstates

We comment here on some of the properties of the eigenstates which are essential to our treatment. These properties stem from those of the Bessel functions.

As the applied field increases, the argument of the Bessel function, $z = 2t/\tilde{f}$, decreases. The Bessel functions of the first kind vanish for vanishing argument with the exception of J_0 which goes to one. More specifically, the asymptotic behavior [18] is

$$\lim_{z \to 0} J_\nu(z) = \frac{(z/2)^\nu}{\nu!}. \tag{3.39}$$

So the magnitude of the expansion coefficient,c_ℓ^n, vanishes rapidly as we move away from $\ell = n$. Only a few neighboring sites contribute significantly. This behavior is in dramatic contrast to that of the eigenstates in the absence of field where the states are extended, namely

$$\epsilon_k = 2t \cos k \qquad c_k = \sum_\ell e^{ik\ell} |\ell\rangle.$$

In the low field regime, $z \to \infty$, the Bessel functions exhibit oscillatory behavior,namely:

$$\lim_{z \to \infty} J_\nu = (2/\pi z)^{1/2} \left[\cos(z - \frac{\nu\pi}{2} - \frac{\pi}{4}) \right]. \tag{3.40}$$

Finally, we should note that the above treatment implied infinitely long systems. Finite systems have been treated in the same formalism [9, 10] and rapid convergence to the infinitely long limit has been obtained. Deviations from the Stark Ladder spectrum were only observed for states at the edge of the band and for weak fields. Also, an open ended chain has been implied here. In the latter study, chains with rigid wall and periodic boundary conditions were compared to almost identical energy spectra except at extremely low values of the field.

3.8 Appendix B: Properties of solutions of the Mathieu equation

We present here those properties of the Mathieu solutions which are pertinent to our discussion in Section 3.5. An extensive treatise on the theory of those functions may be found in Ref. [14]. We consider the standard form of the Mathieu equation, namely

$$u'' + (a - 2q\cos 2z)u = 0$$

where a, q are real parameters and the prime denotes differentiation with respect to the variable z. What makes our problem interesting is that the particular form of the solution depends on the values of a and q, which in the context of Section 3.5 depend on the BOA as well as the applied electric field. We can immediately note that the (a, q) plane is divided in regions of stability and instability as can be seen in Figure 8 of Ref. [14]. A solution is stable if it tends to zero or remains bounded as $z \to \infty$; unstable if it tends to $\pm\infty$. When (a, q) lies exactly upon one of the dividing curves, one of the solutions is neutral and periodic and the second solution is unstable. To ensure normalizable, well behaved eigenfunctions of our Hamiltonian we need to consider only the regions of stable and neutral solutions [19]. The consequence of this is restricted paths for the parameters in the (a, q) plane.

We mention the three cases briefly, focusing in more detail in the stable solutions:

• (a,q) falls in a stable region.

When (a, q) lies between a_{2n}, b_{2n+1}, the two linearly independent solutions are

$$u_1(z) \equiv ce_{2n+\beta}(z, q) = \sum_{r=-\infty}^{\infty} c_m^{2n+\beta} \cos(m + \beta)z$$

$$u_2(z) \equiv se_{2n+\beta}(z, q) = \sum_{r=-\infty}^{\infty} c_m^{2n+\beta} \sin(m + \beta)z \tag{3.41}$$

$$\tag{3.42}$$

where $m = 2r$. When (a, q) lies between (a_{2n+1}, b_{2n+2}), $m = (2r + 1)$ and $2n \to 2n + 1$. c_m are well studied functions of a and q and $0 < \beta < 1$. Although for β

68

irrational the solutions are not periodic, in numerical examples these solutions are always found to be periodic.

$$\beta \approx \left[a - \frac{(a-1)}{[2(a-1)^2 - q^2]} q^2 \right]^{1/2} - m \qquad (3.43)$$

• (a,q) on the dividing curves. One of the solutions is periodic with period π for a_{2n}, b_{2n+2} or 2π for a_{2n+1}, b_{2n+1}. The second solution is unstable.

• (a,q) on an unstable regions both solutions are unstable in the range $-\infty < z < \infty$.

Bibliography

[1] *Nonlinear Optical Properties of Organic Molecules and Crystals,* edited by D.S.Chemla and J. Zyss, (Academic Press, New York, 1987).

[2] *Conjugated Polymers*, edited by J.L. Brédas and R. Silbey, (Kluwer Academic Press, 1991).

[3] S.R. Marder, C.B. Gorman, F. Meyers, J. Perry, G. Bourhill, J.L . Bredas, B.M. Pierce, Science **265**, 632 (1994).

[4] F. Meyers, S.R. Marder, B.M. Pierce, J.L. Bredas, J. Am. Chem. Soc. **116**, 10703 (1994).

[5] H.C. Longuet-Higgins and L. Salem, Proc. Roy. Soc. A, **251**, 172 (1959).

[6] D. Yaron and R. Silbey, Phys. Rev. B **45**, 11655 (1992).

[7] L. Salem, *The Molecular Orbital Theory of Conjugated Systems*, (W.A. Benjamin Inc, Reading, MA), (1966).

[8] A. Heeger, D. Kivelson, J. Schrieffer, W.P. Su, Rev. Mod. Phys. **60**, 78 (1988).

[9] H. Fukuyama, R.A. Bari, H.C. Fogedby, Phys. Rev. B **8**, 5579,(1973).

[10] G. S. Stey and G. Gusman, J. Phys. C **6**, 650 (1973).

[11] E.E. Mendez, F. Agullo-Rueda, J.M. Hong, Phys. Rev. Lett. **60**, 242 6 (1988); J. Bleuse, G. Bastard, P. Voisin, Phys. Rev. Let. **60**, 220 (1 988); K.H. Schmidt, N. Linder, G.H. Döhler, *ibid* **72**, 2769 (1 994); J. Rotvig, A.-P. Jauho, H. Smith, *ibid* **74**, 1831 (1995).

[12] R. Tsu and G. Döhler, Phys. Rev. B **12**, 680 (1975).

[13] F.M. Arscott, *Periodic Differential Equations* (Macmillan Company, New York, 1964) p.121.

[14] N.W. Mclachlan, *Theory and Application of Mathieu Functions* (Dover, New York, 1964)

[15] H.P Mulholland and S. Goldstein, Phil. Mag. **8**, 834 (1929).

[16] I.D.L. Albert, T.J. Marks and M.A. Ratner, J. Phys. Chem. **100**, 9714 (1996).

[17] G. Chen and S. Mukamel, J. Chem. Phys. **103**, 9355 (1995).

[18] M. Abramowitz and H. Stegun, *Handbook of Mathematical Functions* (Dover, New York, 1965).

[19] It is the total wavefunction that needs to be well behaved, but in our case the assymptotic behavior of the Bessel functions $J_\nu(z)$, the only term possible to compensate for the Mathieu solutions unbounded behavior, is $1/z^{1/2}$ slower than the Mathieu solutions $u(z)$ tend to infinity, in particular exponentially in the unstable regions and linearly in the dividing curves.

Chapter 4

Hyper-Rayleigh Scattering of Centrosymmetric Molecules in Solution

4.1 Introduction

Interest in hyper-Rayleigh and hyper-Raman light scattering has been recently revived as an advantageous technique for studying the second order nonlinear response of molecules in solution [1, 2, 3, 4, 5]. The hyper-Rayleigh process of annihilation of two incident photons of frequency ω and the creation of a scattered photon at 2ω is often referred to as incoherent harmonic light scattering (HLS). Similarly, hyper-Raman scattering corresponds to a scattered photon of $2\omega \pm \omega_m$, ω_m being an eigenfrequency of the molecule. Decius and Rauch first proposed the hyper-Raman phenomenon in 1959 [6] which was subsequently observed in the experiments of Terhune, Maker and Savage in 1965 [7]. Since then, selection rules for different symmetry groups, studies of lineshape and the interaction of molecules in solution were discussed, and the experiments and theory were reviewed in Ref. [8]. Interest in this technique waned because of the difficulties in experimental observations.

Experimental improvements and the quest for suitable materials for non linear

optical (NLO) applications motivated a reexamination of this technique. Unlike the most frequently used method of electric-field induced second harmonic generation (EFISHG), it offers the possibility of experimentally measuring the first hyperpolarizability β of molecules with no ground state permanent dipole moment or of ionic molecules in solution. In the first category lies a new class of molecules which are promising candidates for materials for NLO applications: octupolar molecules [1, 9]; in the second category lie synthetic polymers with NLO chromophores and natural proteins [3]. Both categories are of interest for maximizing the microscopic and macroscopic nonlinear response. Unfortunately, EFISHG, the standard technique for the characterization of the first hyperpolarizability of molecules, is limited to dipolar and nonionic species, due to necessity of aligning the molecules in the solvent through their dipole moment by the applied electric field, thus precluding characterization of the above systems. Also, in such an experiment, where the projection of β in the direction of the dipole moment is actually measured, knowledge of both the dipole moment and the second hyperpolarizability γ is necessary to extract information about β. In contrast, HLS experiments on different orientations of polarized light have been used to sort out components of β alone [10, 11, 12]. The advantage becomes then twofold: experimental observation of otherwise inaccessible molecular hyperpolarizabilities of systems of interest and a clean signal without γ contributions.

In the case of centrosymmetric molecules, whose hyperpolarizability vanishes identically in the electric dipole approximation, no hyper-Rayleigh scattering is expected. Nevertheless, intensities at approximately the doubled frequency, 2ω, have been observed for molecules with a center of inversion [13, 14]. The origin of this phenomenon now becomes important if this technique be used for determination of the first hyperpolarizability of molecules. HLS measurements on noncentrosymmetric molecules may then result from contributions other than just that of the first hyperpolarizability.

In this chapter, we focus on hyper-Rayleigh and hyper-Raman scattering of centrosymmetric molecules to elucidate the way hyperpolarizabilities are probed in these processes. The results may then be extended to noncentrosymmetric molecules. In the literature in the late 60's and early 70's, all three interpretations of HLS relied on

cooperative scattering of centrosymmetric molecules or atoms. Kielich suggested that the permanent multipole moments of the neighboring molecules produce a fluctuating field F^i on molecule i, which then lowers the natural symmetry of the molecule and removes its inversion center [13, 15, 16]. Gelbart considered a theory for atomic liquids which included many-body distortion effects so that the signal arises from three-body clusters of atom interactions [17]. Pasmanter *et al.* [18] attributed the phenomenon to the interaction between a dipole induced in one atom and the electric field gradient produced by the dipole induced in an other atom.

Our approach is to discuss a third order effect (involving γ) with the third field produced by the solvent molecules (not necessarily centrosymmetric), which is zero on average. The autocorrelation function of the field due to the reorientation of the solvent molecules determines the light scattering, its strength depending on this correlation function. We propose a twofold contribution: vibrationally induced hyper-Raman and a third order effect involving $\gamma(-2\omega; w, w, 0)$ from the field produced by the solvent molecules. In this case the spectrum of noncentrosymmetric molecules contains β and γ contributions. The relative magnitudes of the two contributions are different and the latter contribution may be negligible with the appropriate choice of solvent. In the case of centrosymmetric solute molecules with a dipolar solvent, the measured intensity will depend on the reaction field strength and the dynamics of the solution and may be used as a probe for such processes.

We express the scattered intensity as the Fourier transform of the appropriate correlation functions. The Heisenberg picture is appealing because it makes an interpretation due to molecular motions possible and enables a classical correspondence to be made. We derive expressions for β and an effective γ from time dependent perturbation theory and then obtain the correlation functions governing the spectral density. In Section 4.2, we study vibrationally induced hyper-Raman for centrosymmetric molecules and in Section 4.3, we study the effect of the effective solvent field in HLS.

4.2 Hyper-Raman scattering: β contribution

In this section we obtain the scattering intensity in terms of the Fourier transform of the correlation function of the appropriate tensor, the hyperpolarizability, β. Since centrosymmetric molecules do not exhibit HLS to this order, we study vibrationally induced hyper-Raman of the ground electronic state as the most relevant to our case. In fact, hyper-Raman scattering around the hyper-Rayleigh line has been experimentally reported [19].

Molecular motions modulate the polarizability. Here, we neglect translational motion; rotations and vibrations of the molecule are considered independently. The lineshape is then connected to the reorientational correlation function and to the vibrational relaxation of the normal modes of appropriate symmetry. Gordon [20] first introduced the reorientational correlation function to study the regular rotational Raman effect. Nafie and Peticolas [21] and Bartoli and Litovitz [22] subsequently included vibrations for the IR, Raman and hyper- Raman effect in one case and Raman in the other. The latter used the semiclassical series expansion for the hyperpolarizability in terms of the normal modes, while the former treated the states quantum-mechanically in the Born-Oppenheimer approximation.

Our treatment applies to an isolated molecule. To treat liquid samples we invoke the following assumptions: isotropic liquids, no angular correlations between molecules separated by distances of the order of the radiation. The dipole approximation will be invoked throughout this chapter. If it may not apply in the sample as a whole, the sample may be divided in scattering volumes whose size is small compared to the scattering wavelength and large over distances of molecular correlations [23, 24]. It is the normalized cross section then that needs to be evaluated. Also, the phases of vibrations in different modes are usually treated as uncorrelated, so the correlation function of the vibrations of different molecules vanishes. No cooperative effects are invoked as explained in Section 4.1

From time dependent perturbation theory, we obtain the most general differential

cross section per molecule to third order (see Appendix A)

$$I(w) \propto d\sigma/d\Omega = \sum_i \rho_i \sum_f |<i^r|\epsilon^3 \cdot \beta : \epsilon^2\epsilon^1|f^r>|^2\delta(\omega_{fi} + \omega_{FI}). \qquad (4.1)$$

where β is the matrix element of the electronic polarizability tensor as a function of the nuclear coordinates for the initial and final electronic states:

$$\beta = \sum_{n,m} \frac{<f|\mu \cdot \epsilon^3|n><n|\mu \cdot \epsilon^2|m><m|\mu \cdot \epsilon^1|i>}{(\omega_{in} - (\omega_{k1} + \omega_{k2}))(\omega_{mi} - \omega_{k1})} + 5 \quad \text{terms.} \qquad (4.2)$$

Throughout the chapter, we use lower-case letters to denote molecular states and upper-case letters to describe the electromagnetic field states. $|i>$ and $|f>$ are the initial and final vibronic states of the scatterer. In the case of a noncentrosymmetric molecule, $|i>=|f>$. For a centrosymmetric molecule, a transition to a normal mode of the ground electronic state with appropriate symmetry is considered. $|i^r>$ and $|f^r>$ correspond to the rotational states, independent of the vibronic states. Before scattering, the sample is assumed to be in equilibrium so the initial states obey a Boltzmann distribution. $\omega \equiv \omega_{FI}$ is the frequency difference between the scattered photon (ω_3 with polarization ϵ_3) and the incident photons (ω_1, ϵ_1, and ω_2, ϵ_2). In our case, (in an HLS experiment), $\omega_1 = \omega_2; \epsilon_1 = \epsilon_2$, and the tensor is symmetric with respect to exchange of the last two indices only. As long as the incident and scattered light frequencies fall away from absorptions, the tensor is usually taken as symmetric. The validity of this approximation is discussed in Ref. [25] where selection rules are obtained for the nonsymmetric case.

To proceed, we will separate the nuclear and electronic motion according to the Born-Oppenheimer approximation and express the wavefunctions in the Herzberg-Teller expansion. Our treatment will be valid for the nonresonant case only so that intermediate vibrational states may be summed. Also, we restrict our interest to transitions for which both the initial and final vibrational states lie in the nondegenerate ground electronic state.

76

We now express the scattering cross section in terms of the relevant correlation functions. We first convert the delta function to its Fourier integral representation

$$\delta(\omega) = \frac{1}{2\pi} \int_{-\infty}^{\infty} dt \exp(i\omega t). \tag{4.3}$$

and substitute it in Eq. 4.1:

$$d\sigma/d\Omega \propto \frac{1}{2\pi} \sum_i \rho_i \sum_f < i|\boldsymbol{\epsilon}^3 \cdot \boldsymbol{\beta} : \boldsymbol{\epsilon}^2\boldsymbol{\epsilon}^1|f > < f|\boldsymbol{\epsilon}^3 \cdot \boldsymbol{\beta} : \boldsymbol{\epsilon}^2\boldsymbol{\epsilon}^1|i >$$

$$\times \int_{-\infty}^{\infty} dt \exp\left[i(\omega_{FI} + \omega_f - \omega_i)t\right]. \tag{4.4}$$

Expressing the energies $\hbar\omega_i$ and $\hbar\omega_f$ as eigenvalues of the Hamiltonian H acting on the initial and final states respectively, and summing over all the final states, we obtain

$$d\sigma/d\Omega \propto \sum_i \rho_i \sum_f \frac{1}{2\pi} \int_{-\infty}^{\infty} dt \exp(i\omega_{FI}t) \tag{4.5}$$

$$\times < i|\boldsymbol{\epsilon}^3 \cdot \boldsymbol{\beta} : \boldsymbol{\epsilon}^2\boldsymbol{\epsilon}^1 \exp(iHt/h)\boldsymbol{\epsilon}^3 \cdot \boldsymbol{\beta} : \boldsymbol{\epsilon}^2\boldsymbol{\epsilon}^1 \exp(-iHt/h)|i > .$$

By defining the quantum mechanical operator, $\hat{\boldsymbol{\beta}}$

$$\hat{\boldsymbol{\beta}}(t) = \exp(iHt/h)\hat{\boldsymbol{\beta}}(0) \exp(-iHt/h)$$

so that it obeys the Heisenberg equation of motion, and denoting the statistical average by brackets $<>$, Eq. 4.5 reduces to

$$I(w) \propto \frac{1}{2\pi} \int_{-\infty}^{\infty} dt \exp(i\omega_{FI}t) < \left[\boldsymbol{\epsilon}^3 \cdot \hat{\boldsymbol{\beta}}(0) : \boldsymbol{\epsilon}^2\boldsymbol{\epsilon}^1\right] \left[\boldsymbol{\epsilon}^3 \cdot \hat{\boldsymbol{\beta}}(t) : \boldsymbol{\epsilon}^2\boldsymbol{\epsilon}^1\right] > \tag{4.6}$$

If the average is interpreted in the classical sense, the classical description is recovered. In the quantum case the ordering of the operators is significant. By neglecting translations the time dependence of the tensor β arises only from reorientation of the molecules. The orientational correlation function depends on the symmetry of the molecule and polarization vectors. The averaging may be done using the direction

cosine method or the characteristic rotation matrices (e.g. [26]).

Including the vibrational states may be done using the semiclassical expression for the expansion of the electronic polarizability in terms of the electronic polarizability following Placzeck, namely

$$\beta(t) = \beta^0(t) + \sum_\nu \partial\beta(t)/\partial q^\nu(t)|_{q=0} q^\nu(t)$$

or the Herzberg- Teller expansion of the wavefunction such that for an electronic state $|n >$

$$|n> = |n^0> + \sum_{m \neq n} <m^0|\frac{\delta H}{\delta q}|n^0> q|m^0> E^0_{nm}.$$

The comparison between the two approximations has been commented in Ref. [27].

By making the latter substitution, assuming the nonresonant case, and dropping the denominator so summation of intermediate vibrational states is possible, we obtain an effective β, β_{eff} with 24 terms, such as

$$\sum_{n,m,a} < g|\epsilon^1 \cdot \boldsymbol{\mu}|a> < a|\frac{\delta H}{\delta q}|n> < n|\epsilon^2 \cdot \boldsymbol{\mu}|m> < m\epsilon^1 \cdot \boldsymbol{\mu}|g> < f|q|i> \quad .... \quad (4.7)$$

From Eq. 4.7 we can now see that scattering is allowed depending on the symmetry of the normal modes.

Following the similar procedure as above, we obtain an expression containing orientational and vibrational correlation functions:

$$I(\omega) \propto \frac{1}{2\pi} \int_{-\infty}^{\infty} dt \exp(i\omega_{FI}t) < \epsilon^3 \cdot \boldsymbol{\beta}(0) : \epsilon^2 \epsilon^1 \epsilon^3 \cdot \boldsymbol{\beta}(t) : \epsilon^2 \epsilon^1 > < q^\nu(o)q^\nu(t) > \quad (4.8)$$

4.3 Hyper-Rayleigh scattering: γ contribution

Despite identically vanishing β, second-order light scattering from centrosymmetric molecules has been experimentally observed [13, 14]. Both Kielich [15, 16] and

Gelbart [17] have discussed this effect. Both approaches rely on intermolecular interactions in the liquid phase and cooperative scattering from correlations among centrosymmetric molecules or atoms. The symmetry of the molecules is lowered due to either interaction with permanent multipole moments of neighboring molecules or many-body distortion effects from triplet clusters of molecules. Kielich points out that scattering occurs when the center of inversion of the scattering molecules is locally destroyed by a molecular electric field created by the permanent moments of its neighbors. The effect is cooperative in nature, involving pairwise correlations. Gelbart's approach, applied on atomic fluids where the above formalism still fails to explain the scattering, considers the cluster expansion of a many-body χ^2 which depends parametrically on the positions of all the nuclei. The first nonvanishing contribution arises then from triplet cluster terms. Our proposition does not rely on the cooperative effect among centrosymmetric molecules. Rather, we are considering the field, created by solvent molecules (not necessarily centrosymmetric) on a solute molecule - in particular, the single particle autocorrelation function of the field due to reorientation of the solvent molecules. Such a function is expected to vary with solvent. On average, $< F >= 0$, but $< F(0,r)F(t,r') > \neq 0$. Instantaneously, this field exhibits low frequency time dependences (i.e. with Fourier components $\omega_\delta \approx 0$.)

The HLS experiment then depends on the second hyperpolarizability of the molecule (fourth order in perturbation theory) $\gamma(-2\omega; \omega, \omega, 0)$, where the third field is provided by the solvent. The solvent is treated here classically, within the dielectric continuum approach, for simplicity. In this proposed picture, the hyper-Rayleigh scattering from the noncentrosymmetric molecules in solution will then appear as a result of two contributions: β and γ.

To obtain the intensity we follow the same procedure as in Section 4.2. Here we ignore the vibrations. The 4th order perturbation theory expression is given in Appendix B. The cross section is now

$$d\sigma/d\Omega \propto \sum_i \rho_i \sum_f \sum_{\alpha,\beta} \rho_{\alpha\alpha} |\langle i, \alpha_{solv} | \epsilon^3 \cdot \tilde{\gamma} \cdot F : \epsilon^2 \epsilon^1 | f, \beta_{solv} \rangle|^2 \delta(\omega_{fi} + \omega_{FI} + \omega_\delta). \quad (4.9)$$

where F is the solvent field, α and β the initial and final solvent states respectively and $\rho_{\alpha\alpha}$ the equilibrium distribution of the initial solvent states. The important frequencies ω_δ are expected to be small compared to ω and 2ω. Rearranging the above equation in a similar manner to Section 4.2, we obtain

$$d\sigma/d\Omega \propto \frac{1}{2\pi} \int dt \exp(i\omega_{FI}t)\langle\tilde{\gamma}(0)\tilde{\gamma}(t)\rangle\langle F(0)F(t)\rangle \qquad (4.10)$$

where $\langle F(0)F(t)\rangle = \sum_{\alpha,\beta}\rho_{\alpha,\alpha}F_{\alpha\beta}F_{\beta\alpha}(t) = \sum_q F_q F_q^* e^{i\omega_q t}$ and

$$\tilde{\gamma} = \sum_{m,n,\ell}\sum_{\epsilon} \frac{\langle f|\boldsymbol{\mu}\cdot\boldsymbol{\epsilon}|\ell\rangle\langle\ell|\boldsymbol{\mu}\cdot\boldsymbol{\epsilon}^3|n\rangle\langle n|\boldsymbol{\mu}\cdot\boldsymbol{\epsilon}^2|m\rangle\langle m|\boldsymbol{\mu}\cdot\boldsymbol{\epsilon}^1|i\rangle}{(\omega_{li} + (\omega_{k3} - \omega_{k1} - \omega_{k2}))(\omega_{ni} - (\omega_{k1} + \omega_{k2})(\omega_{mi} - \omega_{k1})} + 23\,\text{terms.}$$

$$(4.11)$$

Note that we have averaged over all polarizations in the case of the interaction with the solvent field.

For the HLS experiment, we can express

$$\omega_{FI} = \omega_3 - \omega_2 - \omega_1 = \omega - 2\omega_0,$$

in terms of the incident frequency, ω_0 and the scattered one, ω, so the scattering cross section now becomes

$$d\sigma/d\Omega \propto \frac{1}{2\pi} \int dt\, e^{i(\omega - 2\omega_0)t}\langle\tilde{\gamma}(0)\tilde{\gamma}(t)\rangle\langle F(0)F(t)\rangle \qquad (4.12)$$

4.3.1 The solvent field

In our treatment we include the polarization fluctuations of the solvent. To proceed, we must calculate the solvent field correlation function. The Hamiltonian has thus the additional term of

$$H_{solv} = \sum_i \boldsymbol{\mu}_i \cdot \mathbf{F}$$

where $\boldsymbol{\mu}$ is the dipole moment of particle i and $\mathbf{F} = \mathbf{E}_0$ is the solvent field. We consider a solution of centrosymmetric solute molecules in a dipolar solvent. Our goal is to obtain the low frequency modes of the field created by the solvent molecules. It is

assumed that it is a linear responding dipole field. To this end, we begin by a macroscopic theory, where we first obtain the field components as a function of the dielectric constant of the medium. The solvent is thus modeled as a continuum dielectric, with dielectric constant $\epsilon_2(\omega)$ and volume W, surrounding the solute of volume V and dielectric constant $\epsilon_1(\omega)$. Since the resulting fields are known to be shape dependent, we take the molecular sample to be a sphere of radius α for simplicity. In the reaction field approach, the environment of the molecule in focus is treated as a continuum. The field felt by the molecule, due to the dipole that describes the molecule itself as well as by the interaction of the dipole with the surrounding dielectric is known for a spherical cavity [28].

By direct application of linear response theory, where the response of a system to a weak perturbation is completely described in terms of the time correlation function of the appropriate dynamical property, an approach extensively studied in the context of dielectric relaxation [29], the dielectric constant is related to the appropriate macroscopic correlation function, the dipole moment of the sample.

The polarization, in linear response, is related to the external field through the susceptibility:

$$\mathbf{P}(\omega) = \chi(\omega)\mathbf{E}_0(w). \tag{4.13}$$

The polarization is related to the net dipole moment per unit volume of the system in the presence of $\mathbf{E}_0$

$$\mathbf{P}(\omega)e^{i\omega t} = \frac{1}{V} < \sum \mu_i(t) > \mathbf{E}_0, \tag{4.14}$$

and the susceptibility $\chi(\omega)$ is related to the net dipole moment in the molecular sample, $\mathbf{m}(t) = \sum_i \mu_i(t)$ according to

$$\chi(\omega) = -\frac{\beta}{V} \int_0^\infty dt e^{-i\omega t} \frac{d}{dt} < \mathbf{m}(0)\mathbf{m}(t) >= \beta L[-\frac{d}{dt} < \mathbf{m}(0)\mathbf{m}(t) >]. \tag{4.15}$$

where L denotes the Laplace transform with variable $z = i\omega$.

Also, the polarization in the sample is related to the macroscopic, or internal field of the sample, $\mathbf{E}(w)$ in the following way:

81

$$\mathbf{P}(\omega) = \frac{\epsilon_2(\omega) - 1}{4\pi} \mathbf{E}(w).$$ (4.16)

Before we proceed to the specific examples we chose for illustrative purposes, we note the difference between the external field, $\mathbf{E}_0(\omega)$, which exists in the volume of the sample when the latter is removed from the dielectric medium, and the macroscopic Maxwell field, $\mathbf{E}(w)$, which is the field the sample actually feels. In general, the relationship between the two is complicated; however, simple in the case of a spherical sample in an infinite medium. The solute molecules, or spherical molecular sample experience a field produced by the polarization in the solvent, which has been induced by the polarization in the sample, hence the term reaction field is used to describe the macroscopic field.

By means of simple electrostatic boundary value calculations [30] to a sphere embedded in an infinite dielectric medium for two cases: a) in the presence of a constant electric field and b) and an extended dipole moment inside the polarized sphere, we obtain the spontaneous fluctuations of the solvent field as a function of the dielectric constant of the medium and the geometry of the sample. The applied electric field induces polarization in the solvent, the dielectric medium. When this polarization is caused by the presence of a dipole, which for simplicity lies in a cavity, the field is called the reaction field. We then obtain the fluctuating field of the solvent at that specific place which we put the solute or probe molecule. The probe molecule lies in a cavity just like the solvent molecule. This is the first step towards obtaining truly single particle information where intramolecular interactions and degrees of freedom are explicitly considered for giving rise to fluctuations [31, 32]. In the continuum approach for the environment of the solute molecule, molecular structure of matter and interactions are not taken into account explicitly. Finally, we will use such known results of the single-particle correlation function in our treatment.

Constant electric field $\mathbf{E}_\infty$ We first consider the case of a constant applied electric field $\mathbf{E}_\infty$ present at the medium of dielectric constant $\epsilon_1(\omega)$, at a large distance from the spherical sample of radius α and dielectric constant $\epsilon_2(\omega)$. (Here, we impose the

field of the polarized solute to the solvent. This is a crude first step to treating more realistically the response to the sample polarization in the next section.)

In this case, the external field inside the sphere, $\mathbf{E}_0$, that is the field present in the cavity in the absence of the solute is the one that enters the linear response formalism [33]. From a standard electrostatic calculation [30], this field is

$$\mathbf{E}_0(w) = \frac{3\epsilon_1(\omega)}{2\epsilon_1(\omega) + 1}\mathbf{E}_\infty \tag{4.17}$$

Combining Eq. 4.13, 4.16 and 4.17, we obtain for the field in the sample:

$$\mathbf{E}(\omega) = \frac{4\pi}{\epsilon_2(\omega) - 1}\frac{3\epsilon_1(\omega)}{2\epsilon_1(\omega) + 1}\mathbf{E}_\infty \times \int e^{-i\omega t}\frac{d}{dt} < m(0)m(t) > dt. \tag{4.18}$$

The field outside the sphere is composed of the applied field $\mathbf{E}_\infty$ and a dipolar field of an effective dipole

$$\frac{\epsilon_1(\omega) - \epsilon_2(\omega)}{2\epsilon_1(\omega) + \epsilon_2(\omega)}\mathbf{E}_\infty a^3 \tag{4.19}$$

A point dipole at the center of the cavity Similarly, we consider the case of a point dipole μ inside the sphere. The insertion of a dipole in a polarizable solvent produces a field, R. The reaction field is the field felt by the dipole due to this polarization of the solvent. Again, we treat the solvent particles as a dielectric continuum outside the sphere surrounding the dipole. The dipole, the solvent molecule, lies in a cavity similar to the one of the probe solute molecule. We thus obtain the solvent field that the solute molecule would feel at that point. The macroscopic field $\mathbf{E}(\omega)$ at the sample is now the reaction field, R, which can be obtained from an electrostatic calculation [30]:

$$R(t) = \frac{2}{\epsilon_2(\omega)}\frac{[\epsilon_1(\omega) - \epsilon_2(\omega)]}{[2\epsilon_1(\omega) + \epsilon_2(\omega)]}\frac{\mu(t)}{\alpha^3}. \tag{4.20}$$

For simplicity, the dipole lies in the z axis. The field outside the sphere is again a dipolar field of an effective dipole

$$\frac{3}{2\epsilon_1(\omega) + \epsilon_2(\omega)}\mu.$$ (4.21)

From Eq. 4.20, we obtain

$$\langle R(0)R(t)\rangle = \frac{4}{\alpha^6}\langle\mu(0)\mu(t)\rangle\frac{[\epsilon_1(\omega) - \epsilon_2(\omega)]}{\epsilon_2(\omega)\left[2\epsilon_1(\omega) + \epsilon_2(\omega)\right]} \times \frac{[\epsilon_1^*(\omega) - \epsilon_2^*(\omega)]}{\epsilon_2^*(\omega)\left[2\epsilon_1^*(\omega) + \epsilon_2^*)(\omega)\right]}$$ (4.22)

where $\epsilon^*(\omega)$ is the complex conjugate of the dielectric constant. Computer simulations have been used to obtain forms for the autocorrelation function of the dipole moments [34]. For the behavior of the dipole moment correlation function, we assume here the simplest model: the Debye model of dielectric behavior where the correlation function decays exponentially from its initial value,

$$\langle\mu(0)\mu(t)\rangle \propto e^{-|t|/\tau}.$$ (4.23)

τ is a measure of the duration of the correlation and it is a relaxation time. Also, within the same model, the dielectric constant goes like

$$\epsilon(\omega) = 1 + \frac{\epsilon_0}{1 + i\omega\tau}$$ (4.24)

where

$$\epsilon_0 = \epsilon(0)$$

is the static dielectric.

Since we have assumed that the point dipole lies in a cavity, $\epsilon_2(\omega) = 1$, and combining Eq. 4.22, 4.23 and 4.24 we obtain for irradiation at ω_0

$$\langle R(0)R(t)\rangle = \frac{4}{\alpha^6}\frac{(\epsilon_0 - 1)^2}{(2\epsilon_0 + 1)^2[1 + \omega_0^2\tau^2]}e^{-|t|/\tau}.$$ (4.25)

We are now ready to calculate the total cross section by substituting the form

84

of the solvent correlation function of Eq. 4.25 to our original expression in Eq. 4.12. The γ correlation function will be constant for a specific molecule and experimental setup. The time averaging over the motion of the molecules will involve macroscopic averages of the second hyperpolarizability tensor γ of the form $\langle \gamma_{IJKL} \gamma_{MNKO} \rangle$. Since all molecules, centrosymmetric or not, possess non-zero components, there will be a fixed contribution for each molecule. We can thus study the change in the spectrum from solvent to solvent for a chromophore. For a specific molecule then

$$I(\omega) \propto \frac{4}{2\pi\alpha^6} \frac{(\epsilon_0 - 1)^2}{(2\epsilon_0 + 1)^2 [1 + 2\omega_0^2 \tau^2]} \frac{1/\tau}{(\omega - \omega_0)^2 + (1/\tau)^2}. \tag{4.26}$$

solvent	ϵ_0	τ (ps)
chloroform	4.78	5.4
bromoform	4.39	19
nitrobenzene	34.89	41
quinoline	9	45

Table 4.1: Four representative molecules with a range of dielectric constants and relaxation times are chosen as solvents for a HLS experiment of a centrosymmetric chromophore

For illustrative purposes we choose four quite different solvents, with parameters as shown in Table 4.1. We obtain the lineshapes for frequencies typically used in the experiments in Ref. [2] and a much lower one for comparison as may be seen in Figure 4-1.
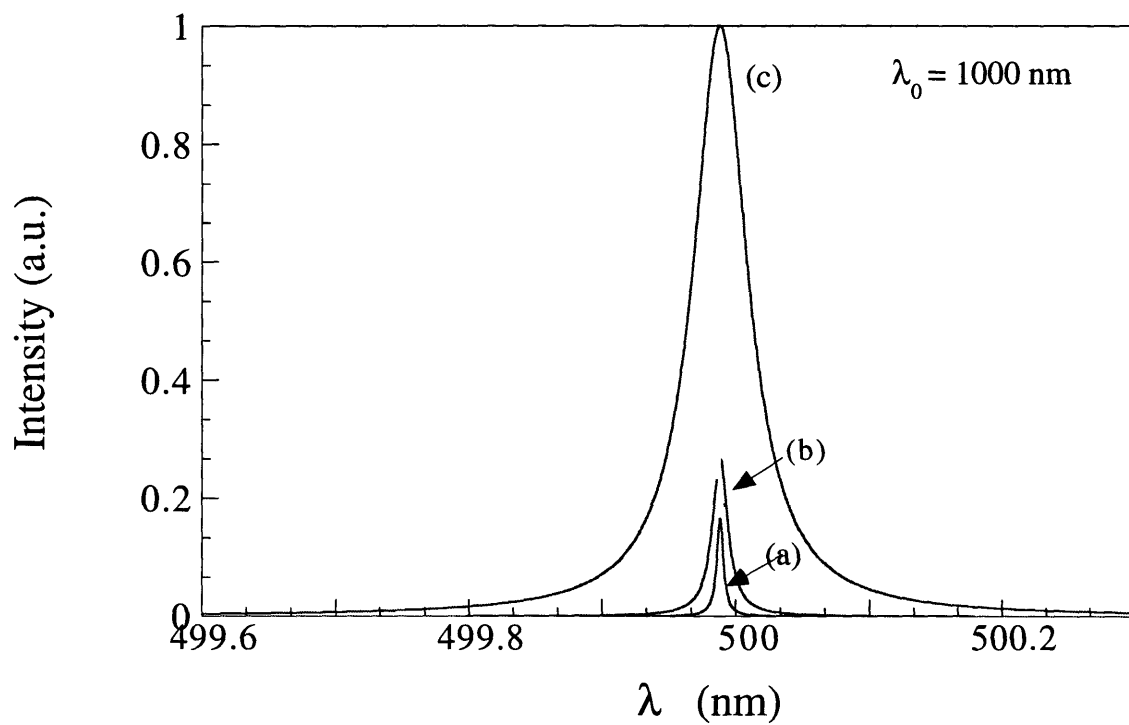
Figure 4-1: HLS of a centrosymmetric chromophore with $\lambda_0 = 1000$ nm typically used in the experiments of Ref. [2] in different solvents: (a) quinoline (b) bromoform (c) chloroform.

4.4 Conclusions

We have considered hyper-Rayleigh and hyper-Raman light scattering of centrosymmetric molecules in solution. We have shown that both processes are possible, even in the presence of identically vanishing β. Especially, in the case of hyper-Rayleigh, we proposed that the contribution is a third order effect involving the second hyperpolarizability γ as well as the dielectric behavior of the solvent. The lineshape then, centered at frequency $2\omega_0$ is Lorentzian at the center, and has its wings clipped. This effect may be important as harmonic light scattering is re-introduced as an advantageous technique to measure the hyperpolarizability β of potentially important materials for nonlinear optics. If it is undesirable, it may be minimized by the appropriate choice of solvent. On the other hand, this technique may be used to probe the solvent reaction fields.
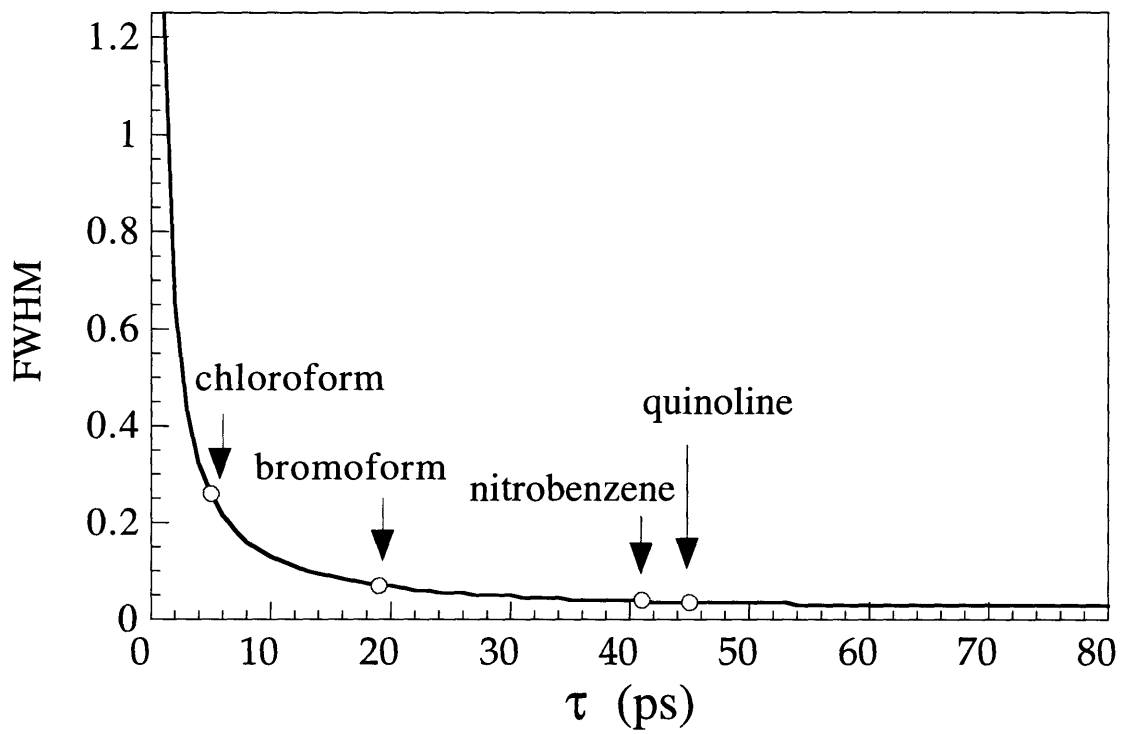
Figure 4-2: The full width at half maximum at scattering frequency $2\omega_0$ as a function of the relaxation time τ of the solvent. The marks correspond to the specific solvents considered.

4.5 Appendix A: HLS cross section

The differential cross section for the "quasi elastic" HLS of centrosymmetric molecules in solution is obtained. The radiation field is treated quantum mechanically. We reserve the capital letter kets for the photon and system states and the lower case letter kets for the system states. So the total differential cross section, $\frac{d\sigma}{d\Omega}$, is equal to

$$\frac{d\sigma}{d\Omega}\Big|_{\mathcal{F}\leftarrow\mathcal{I}} = \frac{V}{cd\Omega}\, T_{\mathcal{F}\leftarrow\mathcal{I}}$$

where $T_{\mathcal{F}\leftarrow\mathcal{I}}$ is the transition rate from the molecular initial state $|I|\rangle$ to the final molecular state $|F\rangle$ and may be obtained from time dependent perturbation theory. c stands for the speed of light and V for the enclosed volume. Now,

$$T_{F\leftarrow I} = \sum_f \rho_f \sum_i \rho_i \frac{|C_{f\leftarrow i}|^2}{t}$$

is related to the transition amplitude $C_{f\leftarrow i}(t)$ from the initial to the final state of the system as well as the density of final and initial states per unit energy per unit volume: ρ_f and ρ_i respectively. We assume that before each photon is scattered the sample has come to equilibrium so that

$$\rho_i = \frac{e^{-\hbar\omega_i/kT}}{\sum_i e^{-\hbar\omega_i/kT}}.$$

The density of final states is given by

$$\rho_f = \frac{d\Omega}{\hbar}\,\frac{w'^2}{(2\pi c)^3}$$

where w' is the frequency of of the scattered photon and $d\Omega$ the solid angle within which lies $\vec{k}'$

We now proceed to calculate the transition amplitude to third order in perturba-

tion theory. Formally,

$$C_{f \leftarrow i}(t)^{(3)} = \frac{1}{(i\hbar)^3} \int_0^t d\tau \langle f|V_I(\tau) \int_0^\tau dt' V_I(t') \int_0^{t'} dt'' V_I(t'')|\Psi_I(0)\rangle \qquad (4.27)$$

V_I is the time dependent part of the Hamiltonian in the interaction representation. In our case,

$$H = H_0 + H(t)$$

where H_0 is given by

$$H_0 = H_{\text{system}} + H_{\text{radiation}}$$

and

$$H(t) = H_{\text{interaction}}.$$

Only the terms which annihilate or create one quantum need be considered and $H_{\text{interaction}} \equiv H(1)$. By inserting complete set of states in Eq. 4.27, we obtain for the transition amplitude of the annihilation of two incident photons of wavevector $\vec{k}_1, \vec{k}_2$ and polarization λ_1, λ_2 and the creation of a photon with wavevector $\vec{k}_3$ and polarization λ_3:

$$
\begin{aligned}
C^{(3)}_{f \leftarrow i}(t)|_{\vec{k}_3 \lambda_3 \leftarrow \vec{k}_2, \lambda_2; \vec{k}_1, \lambda_1} = & \frac{1}{(i\hbar)^3} \sum_{K,L} \int_0^t d_\tau H(1)_{FK} e^{i\omega_{FK}\tau} \int_0^\tau dt' H(1)_{KL} e^{i\omega_{KL}t'} \\
& \int_0^{t'} dt'' H(1)_{LM} e^{i\omega_{LI}t''}.
\end{aligned}
$$

There are 3! possible Feynman diagrams for this process corresponding to the different sequences of annihilation of two quanta, creation of a third quantum. The above sum thus has 6 terms. Looking at carefully one of the terms, namely the annihilation of photon $\vec{k}_1, \lambda_1$ followed by that of photon $\vec{k}_2, \lambda_2$, the emission of $\vec{k}_3, \lambda_3$ we obtain:

$$\text{Term1} \ = \ \frac{-1}{i\hbar} \sum_{k,l} \int_0^t d\tau e^{i\omega_{FI}\tau + i\omega_{fi}\tau} \frac{\langle f|p^{\lambda^3} e^{-i\vec{k}_3 \cdot \vec{r}}|k\rangle}{[\epsilon_k - \epsilon_i - \hbar(\omega_1 + \omega_2)]}$$

$$\frac{\langle k|p^{\lambda^2} e^{-i\vec{k}_2 \cdot \vec{r}}|\ell\rangle}{[\epsilon_\ell - \epsilon_i - \hbar\omega_1]} \langle \ell|p^{\lambda^1} e^{i\vec{k}_1 \cdot \vec{r}}|i\rangle$$

$$\times \ \ (e/m)^3 (2\pi\hbar/cv)^{3/2} \frac{1}{(k_1 k_2 k_3)^{1/2}} n_{k_1}^{1/2} n_{k_2}^{1/2} n_{k_3+1}^{1/2} \tag{4.28}$$

The occupation numbers $n_{k,\lambda}$ are the number of quanta with wavevector $\vec{k}$ and polarization λ; $\omega_{\mathcal{FI}} \equiv \frac{\epsilon_f - \epsilon_i}{\hbar} + \omega_3 - \omega_2 - \omega_1 + \omega_\delta$. The scattering system is constructed by N units each of n_a charged particles which can be regarded as independent of each other. Within each unit the exponentials can be regarded as constants. For $\vec{R}_a$, the vector from an arbitrary origin to a fixed point in the scattering unit a and for $e\langle k|p^{\lambda_i}|m\rangle = im\omega_{km}\langle k|\mu^{\lambda_i}|m\rangle$, Eq. 4.28 becomes

$$\text{Term1} \ = \ \frac{-i}{\hbar} \int_0^t d\tau e^{i\omega_{FI}\tau + i\omega_{fi}\tau} \sum_{a=1}^{N} e^{i\vec{R}_a \cdot (\vec{k}1 + \vec{k}2 - \vec{k}3)} \sum_{k,l} \frac{\langle f|\mu^{\lambda^3}|k\rangle}{[\epsilon_k - \epsilon_i - \hbar(\omega_1 + \omega_2)]}$$

$$\frac{\langle k|\mu^{\lambda^2}|\ell\rangle}{[\epsilon_\ell - \epsilon_i - \hbar\omega_1]} \langle \ell|\mu^{\lambda^1}|i\rangle$$

$$\times \ \ im^3 \omega_{kl}\omega_{lm}\omega_{mi}(e/m)^3 (2\pi\hbar/cv)^{3/2} \frac{1}{(k_1 k_2 k_3)^{1/2}} n_{k_1}^{1/2} n_{k_2}^{1/2} n_{k_3+1}^{1/2} \tag{4.29}$$

4.6 Appendix B

We obtain the differential cross section for the "quasi elastic" HLS of centrosymmetric molecules in solution. We treat the radiation field quantum mechanically and the solvent field classically. We reserve the capital letter kets for the photon and system states and the lower case letter kets for the system states. So the total differential cross section,$\frac{d\sigma}{d\Omega}$, is equal to

$$\frac{d\sigma}{d\Omega}|_{\mathcal{F}\leftarrow\mathcal{I}} = \frac{V}{cd\Omega} T_{F\leftarrow I}$$

where $T_{F \leftarrow I}$ is the transition rate from the initial state $|I\rangle$ to the final state $|F\rangle$ and may be obtained from time dependent perturbation theory. c stands for the speed of light and V for the enclosed volume. Now,

$$T_{F \leftarrow I} = \sum_f \rho_f \sum_i \rho_i \frac{|C_{f \leftarrow i}|^2}{t}$$

is related to the transition amplitude $C_{f \leftarrow i}(t)$ from the initial to the final state of the system as well as the density of final and initial states per unit energy per unit volume: ρ_f and ρ_i respectively. We assume that before each photon is scattered the sample has come to equilibrium so that

$$\rho_i = \frac{e^{-\hbar \omega_i / kT}}{\sum_i e^{-\hbar \omega_i / kT}}.$$

The density of final states is given by

$$\rho_f = \frac{d\Omega}{\hbar} \frac{w'^2}{(2\pi c)^3}$$

where w' is the frequency of of the scattered photon and $d\Omega$ the solid angle within which lies $\vec{k}'$

We now proceed to calculate the transition amplitude to fourth order in perturbation theory. Formally,

$$C_{f \leftarrow i}(t)^{(4)} = \frac{1}{(i\hbar)^4} \int_0^t d\tau \langle f|V_I(\tau) \int_0^\tau dt' V_I(t') \int_0^{t'} dt'' V_I(t'') \int_0^{t''} dt''' V_I(t''')|\Psi_I(0)\rangle \tag{4.30}$$

V_I is the time dependent part of the Hamiltonian in the interaction representation. In our case,

$$H = H_0 + H(t)$$

where H_0 is given by

$$H_0 = H_{\text{system}} + H_{\text{radiation}}$$

and

$$H(t) = H_{\text{interaction}}.$$

Only the terms which annihilate or create one quantum need be considered and $H_{\text{interaction}} \equiv H(1)$.

By inserting complete set of states in Eq. 4.30, we obtain for the transition amplitude of the annihilation of two incident photons of wavevector $\vec{k}_1, \vec{k}_2$ and polarization λ_1, λ_2 and the creation of a photon with wavevector $\vec{k}_3$ and polarization λ_3:

$$C^{(4)}_{f \leftarrow i}(t)|_{\vec{k}_3\lambda_3 \leftarrow \vec{k}_2,\lambda_2;\vec{k}_1,\lambda_1} = \frac{1}{(i\hbar)^4} \sum_{K,L,M} \int_0^t d\tau H_{FK}^{solv} e^{i\omega_{FK}\tau} \int_0^\tau dt' H(1)_{KL} e^{i\omega_{KL}t'}$$

$$\int_0^{t'} dt'' H(1)_{LM} e^{i\omega_{LM}t''} \int_0^{t''} dt''' H(1)_{MI} e^{i\omega_{MI}t'''}.$$

There are 4! possible Feynman diagrams for this process corresponding to the different sequences of annihilation of two quanta, creation of a third quantum and an interaction with the solvent. The above sum thus has 24 terms. Looking at carefully one of the terms, namely the annihilation of photon $\vec{k}_1, \lambda_1$ followed by that of photon $\vec{k}_2, \lambda_2$, the emission of $\vec{k}_3, \lambda_3$ and finally the interaction with the solvent we obtain:

$$\text{Term1} = \frac{-1}{i\hbar} \sum_{k,l,m} \int_0^t d\tau e^{i\omega_{FI}\tau} H_{FK}^{solv}$$

$$\frac{\langle k|p^{\lambda_3} e^{-i\vec{k}_3 \cdot \vec{r}}|\ell\rangle}{[\epsilon_k - \epsilon_i + \hbar(\omega_3 - \omega_1 - \omega_2)]} \frac{\langle \ell|p^{\lambda_2} e^{i\vec{k}_2 \cdot \vec{r}}|m\rangle}{[\epsilon_\ell - \epsilon_i - \hbar(\omega_2 + \omega_1)]} \frac{\langle m|p^{\lambda_1} e^{i\vec{k}_1 \cdot \vec{r}}|i\rangle}{[\epsilon_m - \epsilon_i - \hbar\omega_1]}$$

$$\times \quad (e/m)^3 (2\pi\hbar/cv)^{3/2} \frac{1}{(k_1 k_2 k_3)^{1/2}} n_{k_1}^{1/2} n_{k_2}^{1/2} n_{k_3+1}^{1/2} \tag{4.31}$$

The occupation numbers $n_{k,\lambda}$ are the number of quanta with wavevector $\vec{k}$ and polarization λ; $\omega_{FI} \equiv \frac{\epsilon_f - \epsilon_i}{\hbar} + \omega_3 - \omega_2 - \omega_1 + \omega_\delta$. The scattering system is constructed by N units each of n_a charged particles which can be regarded as independent of each other. Within each unit the exponentials can be regarded as constants. For $\vec{R}_a$, the vector from an arbitrary origin to a fixed point in the scattering unit a and for

$e\langle k|p^{\lambda_i}|m\rangle = im\omega_{km}\langle k|\mu^{\lambda_i}|m\rangle$, Eq. 4.31 becomes

$$\text{Term1} = \frac{-i}{\hbar}\int_0^t d\tau e^{i\omega_{FI}\tau}\sum_{a=1}^N e^{i\vec{R}_a\cdot(\vec{k1}+\vec{k2}-\vec{k3})}\sum_{k,l,m} H_{FK}^{solv}$$

$$\frac{\langle k|\mu^{\lambda_3}|\ell\rangle}{[\epsilon_k - \epsilon_i + \hbar(\omega_3 - \omega_1 - \omega_2)]}\frac{\langle \ell|\mu^{\lambda_2}|m\rangle}{[\epsilon_\ell - \epsilon_i - \hbar(\omega_2 + \omega_1)]}\frac{\langle m|\mu^{\lambda_1}|i\rangle}{[\epsilon_m - \epsilon_i - \hbar\omega_1]}$$

$$\times \quad im^3\omega_{kl}\omega_{lm}\omega_{mi}(e/m)^3(2\pi\hbar/cv)^{3/2}\frac{1}{(k_1k_2k_3)^{1/2}}n_{k_1}^{1/2}n_{k_2}^{1/2}n_{k_3+1}^{1/2} \qquad (4.32)$$

Now, we substitute for H^{solv}

$$H^{solv} = \mu \cdot F$$

so that

$$H_{fk}^{solv} = \sum_\lambda \langle f|\mu^\lambda|k\rangle \cdot F.$$

Also,

$$I(\omega_i) = n_{k_i}c/V$$

Combining all the above, the scattering cross section becomes

$$\frac{d\sigma}{d\Omega} = \frac{2\pi\hbar}{c^5}\frac{\omega_3}{\omega_1\omega_2}I(\omega_1)I(\omega_2)\sum_f\sum_i \rho_i\left|\sum_{a=1}^N e^{i\vec{R}_a\cdot(\vec{k1}+\vec{k2}-\vec{k3})}\right.$$

$$\times \sum_{k,l,m}\sum_\lambda \frac{\langle k|\mu^{\lambda_3}|\ell\rangle}{[\epsilon_k - \epsilon_i + \hbar(\omega_3 - \omega_1 - \omega_2)]}\frac{\langle \ell|\mu^{\lambda_2}|m\rangle}{[\epsilon_\ell - \epsilon_i - \hbar(\omega_2 + \omega_1)]}\frac{\langle m|\mu^{\lambda_1}|i\rangle}{[\epsilon_m - \epsilon_i - \hbar\omega_1]}$$

$$\left.\cdot F^2\omega_{kl}\omega_{lm}\omega_{mi} + 23 \quad \text{terms}\right|^2 \delta(\omega_f - \omega_i + \omega_3 - \omega_2 - \omega_1 + \omega_\delta) \qquad (4.33)$$

Bibliography

[1] J. Zyss, T. Chau Van, C. Dhenaut, I. Ledoux, Chem. Phys. **177**, 281 (1993); J. Zyss and I. Ledoux, Chem. Rev. **94**, 77 (1994).

[2] P. Kaatz and D.P Shelton, Rev. Sci. Instrum. **67**, 1438 (1996); *ibid*, J. Chem. Phys. **105**, 3918 (1996); *ibid*, Mol. Phys. **88**, 683 (1996).

[3] K. Clays, A. Persoons, L. De Maeyer, in *Advances in Chemical Physics*, ed. by M. Evans and S. Kielich, (Wiley, New York, 1994), Vol. 85, p. 455.

[4] K. Clays and A. Persoons, Phys. Rev. Lett. **66**, 2980 (1991).

[5] G.J.T. Heesink, A.G.T. Ruiter, N.F. van Hulst, B. Bolger, Phys. Rev. Lett. **71**, 999 (1993).

[6] J.C. Decius and J.E. Rauch, *Ohio State Symp. Mol. Spectrosc., Columbus*, Pap.48 (1959).

[7] R.W. Terhune, P.D. Maker, C.M. Savage, Phys. Rev. Lett. **14**, 681 (1965).

[8] M.J. French, Hyper Rayleigh and Hyper Raman Spectroscopy, in *Chemical Applications of Raman Spectroscopy*, (Academic Press, New York, 1981); S. Kielich, Prog. Opt. **20**, 155 (1983) and references therein.

[9] J. Zyss, Nonlinear Optics **1**, 3 (1991).

[10] R. Bersohn, Y.-H. Pao, H.L. Frisch, J. Chem. Phys. **45**, 3184,(1965).

[11] S.J. Cyvin, J.E. Rauch, J.C. Decius, J. Chem. Phys. **43**, 4083 (1965).

[12] G.J.T. Heesink, A.G.T. Ruiter, N.F. van Hulst, B. Bölger, Phys. Rev. Lett. **71**, 999 (1993).

[13] S. Kielich, J.R. Lalanne, F.B. Martin, Phys. Rev. Lett. **26**, 1295 (1971).

[14] W.J. Schmid and H.W. Schrotter, Chem. Phys. Lett. **45**, 502 (1977).

[15] S. Kielich, M. Kozierowski, J.R. Lalanne, Journal de Physique **36**, 1015 (1975).

[16] S. Kielich and M. Kozierowski, Acta Phys. Pol. A **45**, 231 (1974).

[17] W.M. Gelbart, Chem. Phys. Lett. **23**, 53 (1973).

[18] R.A. Pasmanter, R. Samson, and A. Ben-Reuven, Phys. Rev. A **14**, 1238 (1976).

[19] T.J. Dines, M.J. French, R.J.B. Hall and D.A. Long, J. Raman Spectrosc. **14**, 225 (1983).

[20] R.G. Gordon, J. Chem. Phys. **42**, 3658 (1965); *ibid* **43**, 1307 (1965).

[21] L.A. Nafie and W.L. Peticolas, J. Chem. Phys. **57**, 3145 (1972).

[22] F.J Bartoli and T.A. Litovitz, J. Chem. Phys. **56**, 413 (1972).

[23] R.G. Gordon, J. Chem. Phys. **40**, 1973 (1965).

[24] L.D. Landau, E.M. Lifshitz, L.P. Pitaevskii, *Electrodynamics of Continuous Media*, (Pergamon Press, New York, 1984), par. 117.

[25] J.H. Christie and D.J. Lockwood, J. Chem. Phys. **54**, 1141 (1971).

[26] W.A. Steele, *Adv. Chem. Phys.* **34**, 1 (1976).

[27] W.L. Peticolas, L.Nafie, P. Stein, B. Fanconi, J. Chem. Phys. **52**, 1576 (1970).

[28] C.J.F. Böttcher, *Theory of Electric Polarization*, (Elsevier Pub. Co., 1973).

[29] S.A. Adelman and J.M. Deutch, *Adv. Chem. Phys.*, ed. by I. Prigogine and S.A. Rice, (Wiley, New York, 1975), Vol. 31, p. 103, and references therein.

[30] H. Fröhlich, *Theory of Dielectrics*, (Oxford University Press, 1958).

[31] D. Kivelson and P. Madden, Mol. Phys. **30**, 1749 (1975).

[32] L.R. Pratt, Mol. Phys. **40**, 347 (1980).

[33] U.M. Titulaer and J.M. Deutch, J. Chem. Phys. **60**, 1502 (1974).

[34] B.J. Alder and E. L. Pollock, *Ann. Rev. Phys. Chem.* **32**, 311 (1981).